

1 **Supplementary Information**

2

3 **The AAA+ chaperone VCP disaggregates Tau fibrils and generates**  
4 **aggregate seeds in a cellular system**

5 Itika Saha<sup>1,2</sup>, Patricia Yuste-Checa<sup>1,2</sup>, Miguel Da Silva Padilha<sup>3,4,7</sup>, Qiang Guo<sup>5,#</sup>, Roman  
6 Körner<sup>1</sup>, Hauke Holthausen<sup>1</sup>, Victoria A. Trinkaus<sup>1,5,6</sup>, Irina Dudanova<sup>3,4,7</sup>, Rubén Fernández-  
7 Busnadiego<sup>2,5,8,9</sup>, Wolfgang Baumeister<sup>5</sup>, David W. Sanders<sup>10,‡</sup>, Saurabh Gautam<sup>1,§</sup>, Marc I.  
8 Diamond<sup>10</sup>, F. Ulrich Hartl<sup>1,2,6,\*</sup> and Mark S. Hipp<sup>1,6,11,12\*</sup>

9 <sup>1</sup>Department of Cellular Biochemistry, Max Planck Institute of Biochemistry, Am Klopferspitz  
10 18, 82152 Martinsried, Germany.

11 <sup>2</sup>Aligning Science Across Parkinson's (ASAP) Collaborative Research Network, Chevy Chase,  
12 MD, USA.

13 <sup>3</sup>Molecular Neurodegeneration Group, Max Planck Institute for Biological Intelligence,  
14 82152 Martinsried, Germany.

15 <sup>4</sup>Department of Molecules – Signaling – Development, Max Planck Institute for Biological  
16 Intelligence, Am Klopferspitz 18, 82152 Martinsried, Germany.

17 <sup>5</sup>Department of Structural Molecular Biology, Max Planck Institute of Biochemistry, Am  
18 Klopferspitz 18, 82152 Martinsried, Germany.

19 <sup>6</sup>Munich Cluster for Systems Neurology (SyNergy), Munich, Germany.

20 <sup>7</sup>Center for Anatomy, Faculty of Medicine and University Hospital Cologne, University of  
21 Cologne, 50931 Cologne, Germany.

22 <sup>8</sup>Institute of Neuropathology, University Medical Center Göttingen, 37099 Göttingen, Germany.

23 <sup>9</sup>Cluster of Excellence “Multiscale Bioimaging: from Molecular Machines to Networks of  
24 Excitable Cells” (MBExC), University of Göttingen, Germany.

25 <sup>10</sup>Center for Alzheimer's and Neurodegenerative Diseases, Peter O'Donnell Jr. Brain Institute,  
26 University of Texas Southwestern Medical Center, Dallas, 75390 Texas, USA.

27 <sup>11</sup>School of Medicine and Health Sciences, Carl von Ossietzky University Oldenburg,  
28 Oldenburg, Germany.

29 <sup>12</sup>Department of Biomedical Sciences of Cells and Systems, University Medical Center  
30 Groningen, University of Groningen, Antonius Deusinglaan, 1, 9713 AV Groningen, The  
31 Netherlands.

32

33 # Present address: State Key Laboratory of Protein and Plant Gene Research, School of Life  
34 Sciences and Peking-Tsinghua Center for Life Sciences, Peking University, Beijing 100871,  
35 China.

36 ‡ Present address: Department of Chemical and Biological Engineering, Princeton University,  
37 Princeton, NJ 08544, USA

38 § Present address: Boehringer Ingelheim International GmbH, 55216 Ingelheim, Germany and  
39 ViraTherapeutics GmbH, 6063 Rum, Austria.

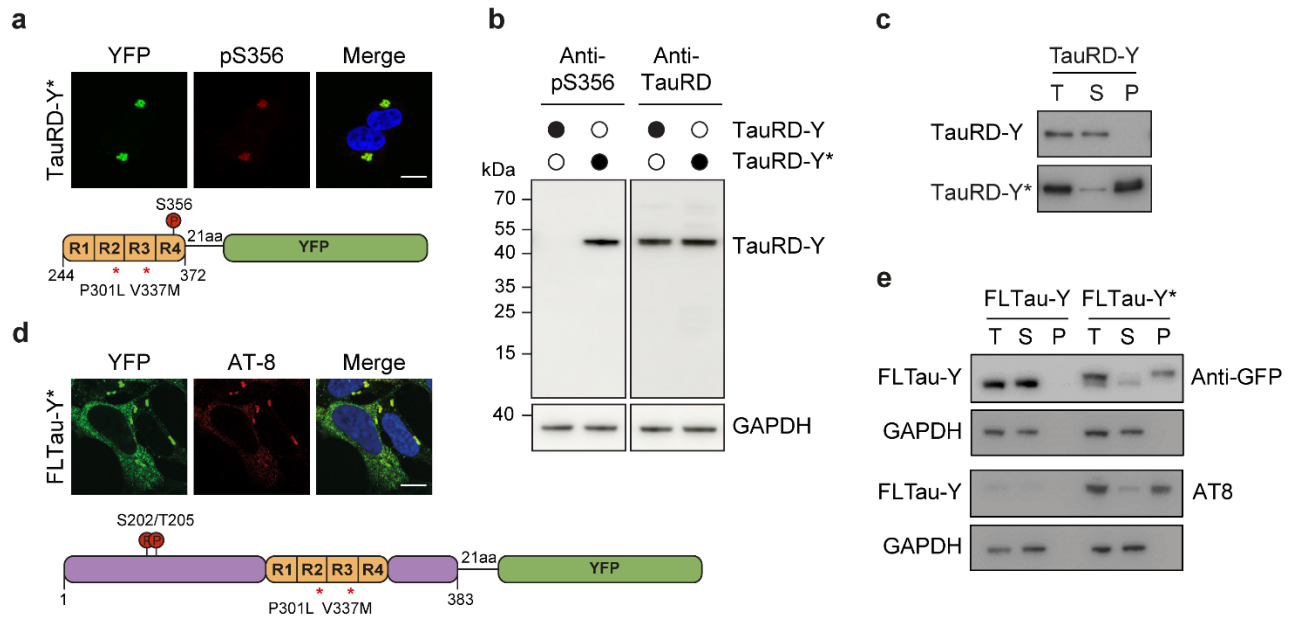
40

41 \*Correspondence to [uhartl@biochem.mpg.de](mailto:uhartl@biochem.mpg.de) and [m.s.hipp@umcg.nl](mailto:m.s.hipp@umcg.nl)

42

43 Supplementary information includes 13 Supplementary Figures, Supplementary Table 1 and  
44 uncropped scans of blots presented in supplementary figures.

45



46

47 **Supplementary Fig. 1: Tau aggregation in a constitutive expression model.**

48 **a** Immunofluorescence staining of TauRD-Y\* cells with an antibody against Tau phosphorylation

49 at S356 (red) and YFP fluorescence of TauRD-Y (green). Scale bar, 10  $\mu$ m. **b** Analysis of Tau

50 S356 phosphorylation in lysates of TauRD-Y and TauRD-Y\* cells by immunoblotting. Total

51 TauRD-Y was detected using antibody against TauRD. **c** Solubility of TauRD-Y in TauRD-Y and

52 TauRD-Y\* cells at steady state, determined by fractionation of cell lysate by centrifugation,

53 followed by immunoblotting with anti-GFP antibody. T, total cell lysate, S, supernatant, P, pellet.

54 **d** Immunofluorescence staining of full-length Tau (FLTau-Y) in aggregate-containing FLTau-Y\*

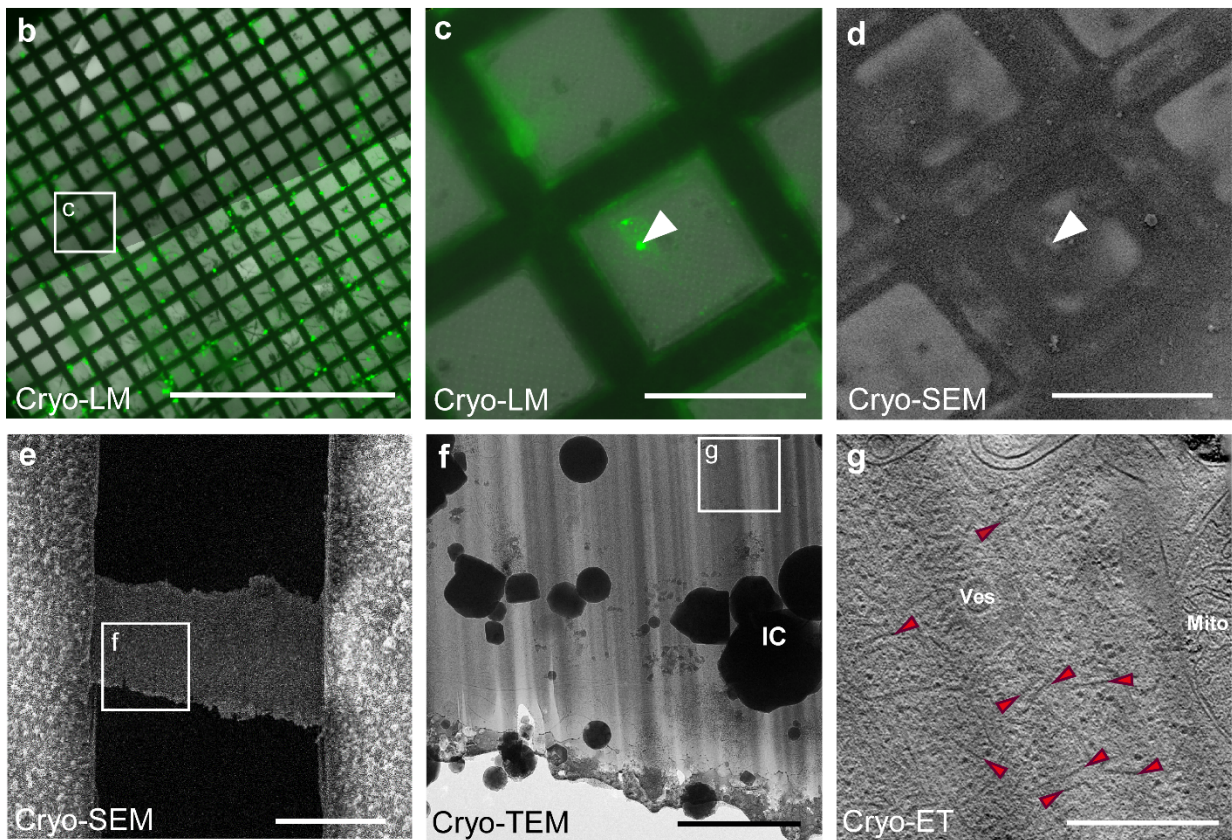
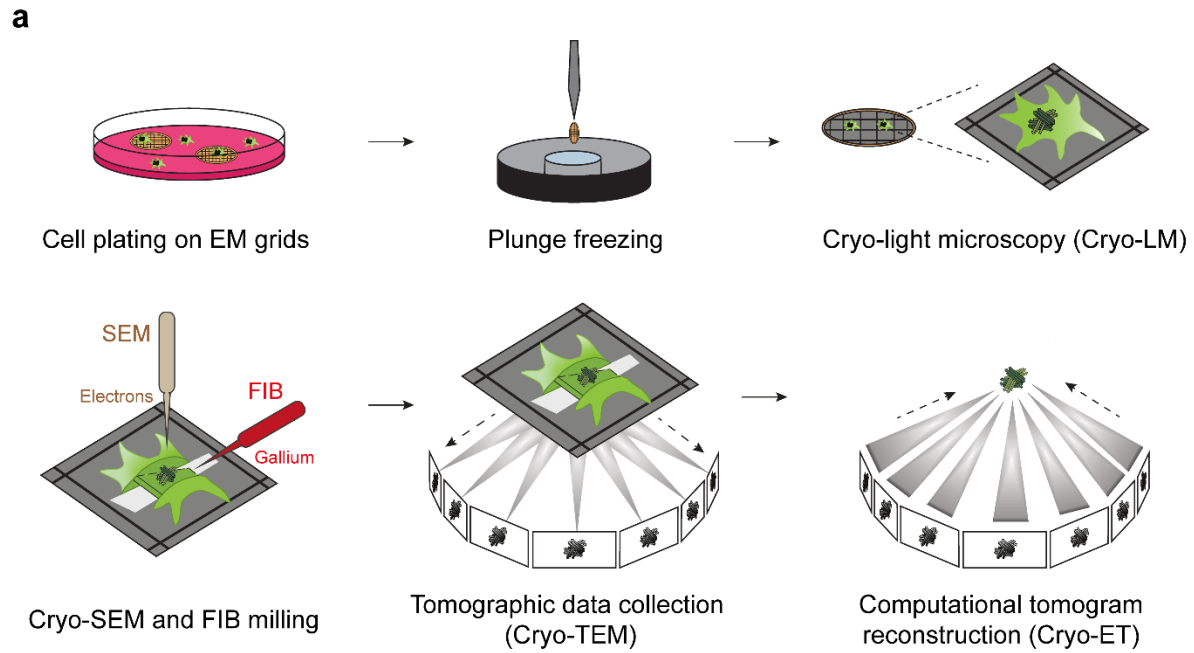
55 cells with AT-8 antibody specific for Tau phosphorylation at S202/T205 (red) and YFP

56 fluorescence of TauRD-Y (green). Scale bar, 10  $\mu$ m. **e** Solubility of phosphorylated FLTau-Y in

57 FLTau-Y and FLTau-Y\* cells at steady state analyzed as in (c). Immunoblotting was with AT-8

58 antibody (bottom) and anti-GFP (top). GAPDH served as loading control.

59



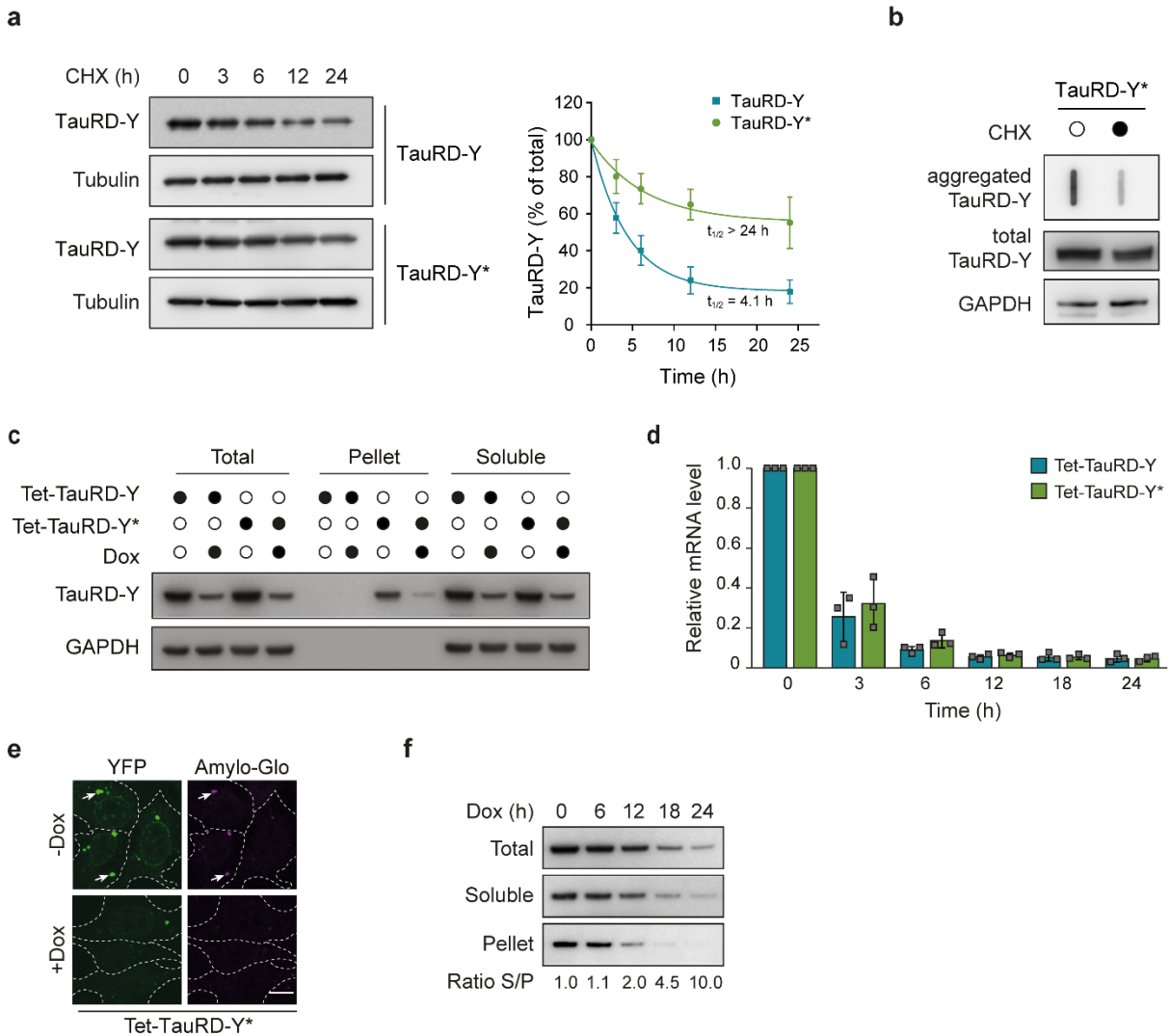
60

61 **Supplementary Fig. 2: Cryo-correlative-light-electron microscopy (cryo-CLEM) workflow.**

62 **a** Schematic representation of the cryo-CLEM workflow on cells containing TauRD-Y aggregates.

63 Cryo-LM (cryo-light microscopy), cryo-SEM (cryo-scanning electron microscopy), cryo-FIB

64 (focused ion beam), cryo-TEM (cryo-transmission electron microscopy), cryo-ET (cryo-electron  
65 tomography). **b** Mouse primary neurons were cultured on EM grids for 10 days and transduced  
66 with TauRD-Y followed by treatment with aggregate-containing cell lysates. 6 days after  
67 transduction, grids were vitrified by plunge freezing. Thereafter, grids were imaged by cryo-light  
68 microscopy (cryo-LM). An image of a grid with neurons containing aggregates is shown. Scale  
69 bar, 1 mm. **c** Zoomed in cryo-LM image of the area marked in (b) by a white box. The arrowhead  
70 indicates a neuronal TauRD-Y inclusion. Scale bar, 100  $\mu\text{m}$ . **d** EM grids were transferred into the  
71 cryo-FIB/SEM. Cryo-SEM image of the area shown in (c). The arrowhead indicates the same  
72 location of the area shown in (c). Scale bar, 100  $\mu\text{m}$ . **e** A  $\sim$ 200 nm thick lamella was generated at  
73 that location by cryo-FIB milling. Scale bar, 10  $\mu\text{m}$ . **f** Cryo-TEM overview of the lamella region  
74 marked in (e). IC: Ice crystal. Scale bar, 2  $\mu\text{m}$ . **g** 1.4 nm thick tomographic slice of a neuronal  
75 TauRD-Y inclusion recorded in the area marked in (f). Red arrowheads indicate representative  
76 TauRD-Y fibrils. Ves: Vesicle, Mito: Mitochondrion. Scale bar, 500 nm.



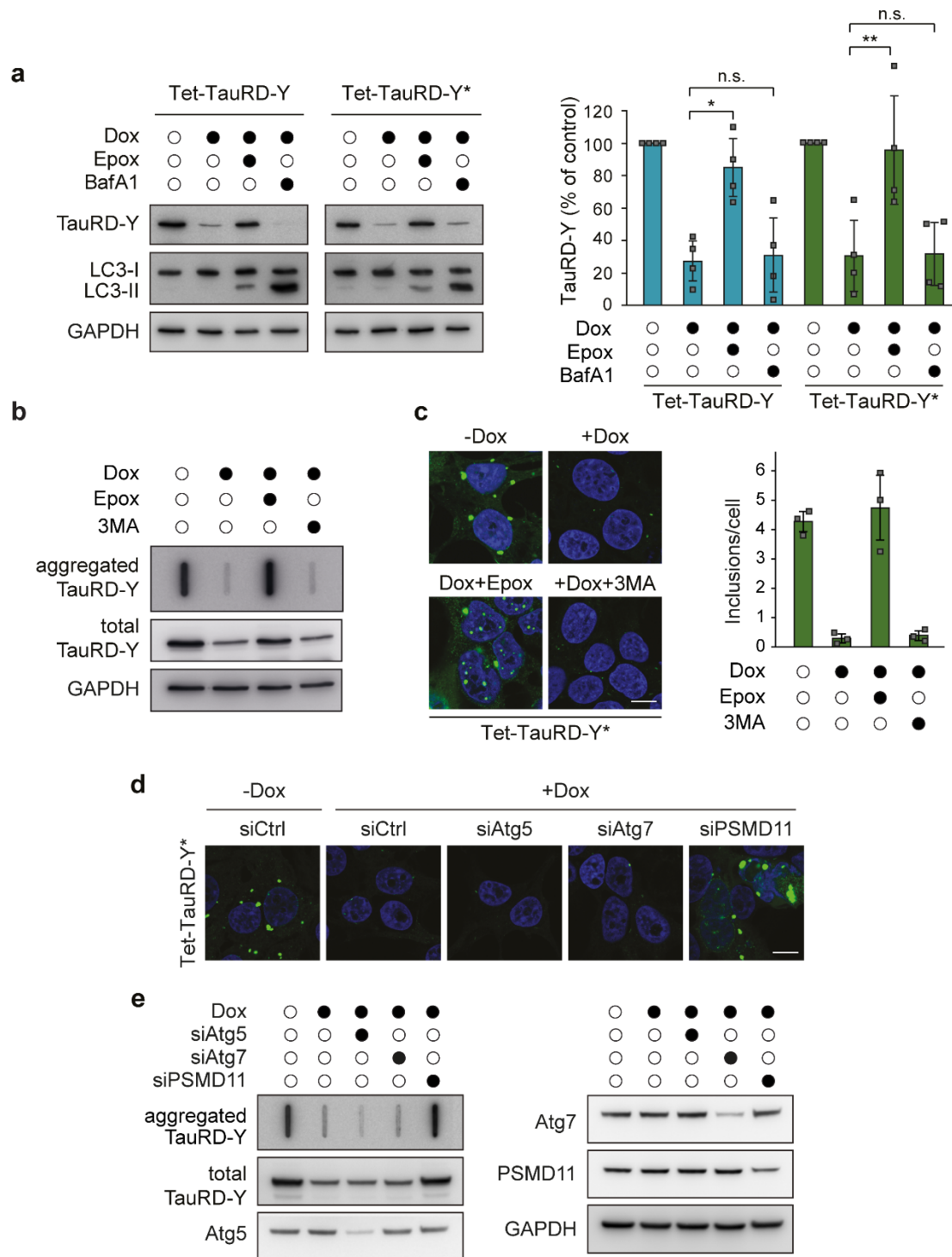
77

78 **Supplementary Fig. 3: TauRD-Y aggregation and clearance upon inhibition of expression in**  
 79 **a constitutive and Tet-regulated TauRD-Y expression system.**

80 **a** Turnover of TauRD-Y in TauRD-Y and TauRD-Y\* cells upon cycloheximide (CHX) shut-off  
 81 (CHX; 50  $\mu$ g/mL). Left, anti-GFP immunoblots to determine TauRD-Y levels. Tubulin served as  
 82 loading control. Right, exponential fits of CHX chase data and corresponding half-lives ( $t_{1/2}$ ).  
 83 Mean  $\pm$  s.d.; n=3. **b** Filter trap analysis of aggregated TauRD-Y upon CHX chase for 24 h.  
 84 Aggregated and total TauRD-Y levels were determined by anti-GFP immunoblotting. GAPDH  
 85 served as loading control. **c** Solubility of TauRD-Y in Tet-TauRD-Y and Tet-TauRD-Y\* cells  
 86 upon addition of 50 ng/mL doxycycline (Dox) for 24 h. Cell lysates were fractionated as in

87 Supplementary Fig. 1c. TauRD-Y was detected with anti-GFP antibody. GAPDH served as  
88 loading control. **d** Quantitative PCR analysis of TauRD-Y mRNA in Tet-TauRD-Y and Tet-  
89 TauRD-Y\* cells treated with Dox for 0, 3, 6, 12, 18 and 24 h. mRNA levels were normalized to  
90 the reference gene *RPS18*. Mean  $\pm$  s.d.; n=3. **e** Representative fluorescence images of Tet-TauRD-  
91 Y\* cells treated with Dox for 24 h showing staining of TauRD-Y inclusions (green) with Amylo-  
92 Glo (magenta). White dashed lines indicate cell boundaries. Scale bar, 10  $\mu$ m. **f** Solubility of  
93 TauRD-Y in Tet-TauRD-Y\* cells upon addition of Dox for the indicated times. Normalized ratios  
94 of TauRD-Y in soluble (S) and pellet (P) fractions are stated. Source data are provided as a Source  
95 Data file.

96



97

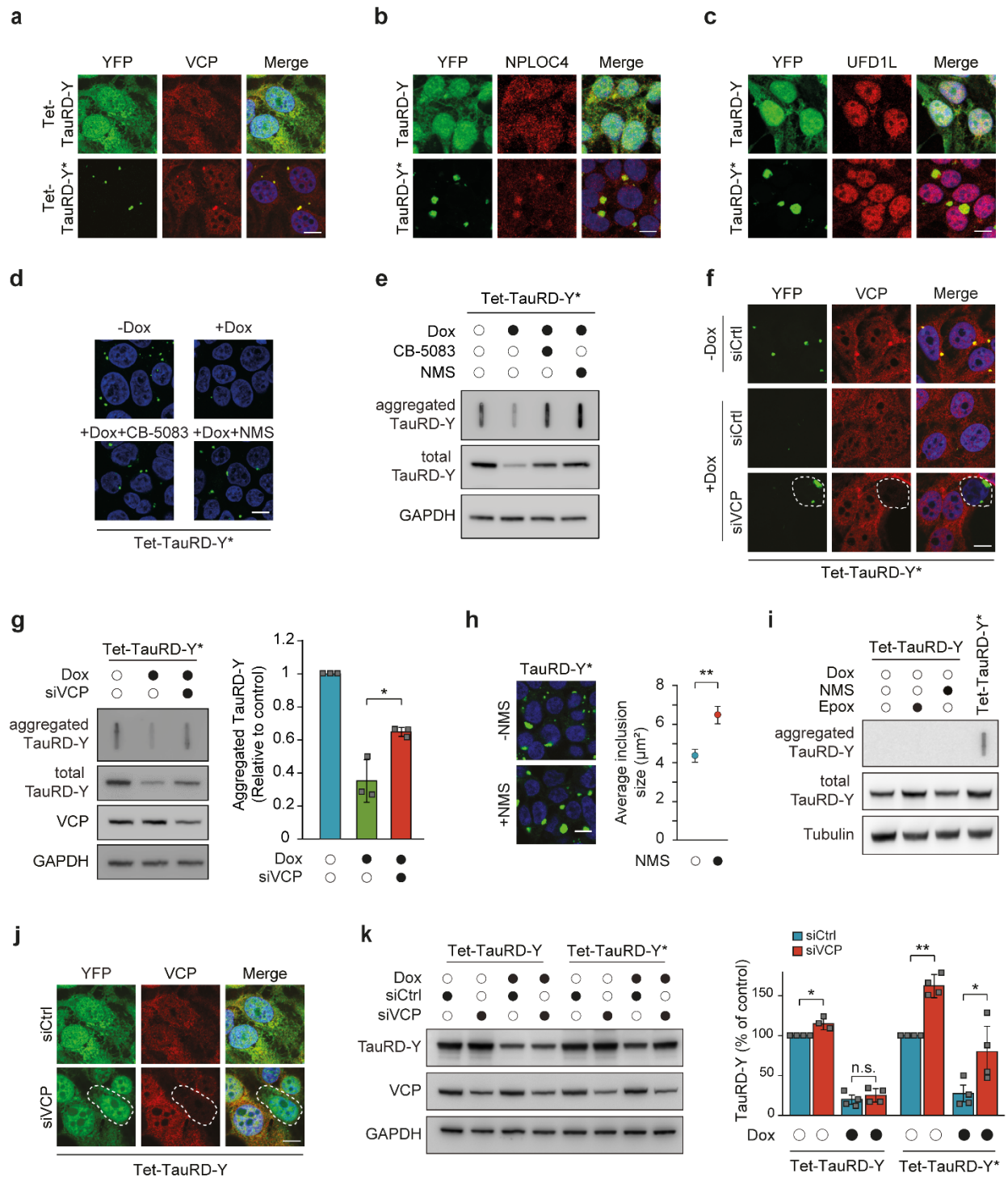
98 **Supplementary Fig. 4: Effect of UPS and autophagy inhibition on TauRD-Y levels and**

99 **aggregate clearance.**

100 **a** Analysis of TauRD-Y levels in Tet-TauRD-Y and Tet-TauRD-Y\* cells treated for 24 h with

101 doxycycline (Dox; 50 ng/mL) alone or in combination with Epoxomicin (Epox; 50 nM) or

102 Bafilomycin A1 (BafA1; 50 nM). TauRD-Y and LC3 levels were determined by immunoblotting  
103 against GFP and LC3B respectively. GAPDH served as loading control. Mean  $\pm$  s.d.; n=4. \*p<0.05  
104 (Tet-TauRD-Y: + Dox vs + Dox + Epox, p=0.0114), \*\*p<0.01 (Tet-TauRD-Y\*: + Dox vs + Dox  
105 + Epox, p=0.0026); n.s. non-significant (Tet-TauRD-Y: + Dox vs + Dox + Epox, p= 0.6422; Tet-  
106 TauRD-Y\*: + Dox vs + Dox + Epox, p= 0.8799) from two-tailed Student's paired t-test. **b** Filter  
107 trap analysis of Tet-TauRD-Y\* cells treated for 24 h with Dox alone or in combination with  
108 Epoxomicin (Epox; 50 nM) or 3-methyladenine (3MA; 5 mM). Aggregated and total TauRD-Y  
109 was detected with anti-GFP antibody. **c** Left, representative images of Tet-TauRD-Y\* cells treated  
110 for 24 h with Dox alone or, in combination with Epoxomicin (Epox; 50 nM) or 3MA (5 mM).  
111 Scale bar, 10  $\mu$ m. Right, quantification of TauRD-Y foci. 100-200 cells analyzed per experiment.  
112 Mean  $\pm$  s.d.; n=3. **d** Representative images of Tet-TauRD-Y\* cells transfected with non-targeted  
113 (Ctrl) siRNA or siRNA against Atg5 (50 nM), Atg7 (50 nM) and PSMD11 (25 nM). 72 h after  
114 transfection, doxycycline (Dox; 50 ng/mL) was added for another 24 h where indicated. Scale bar,  
115 10  $\mu$ m. **e** Filter trap analysis of Tet-TauRD-Y\* cells transfected with siRNAs and treated with Dox  
116 as stated in (d). TauRD-Y was detected by immunoblotting with anti-GFP antibody. Source data  
117 are provided as a Source Data file.



118

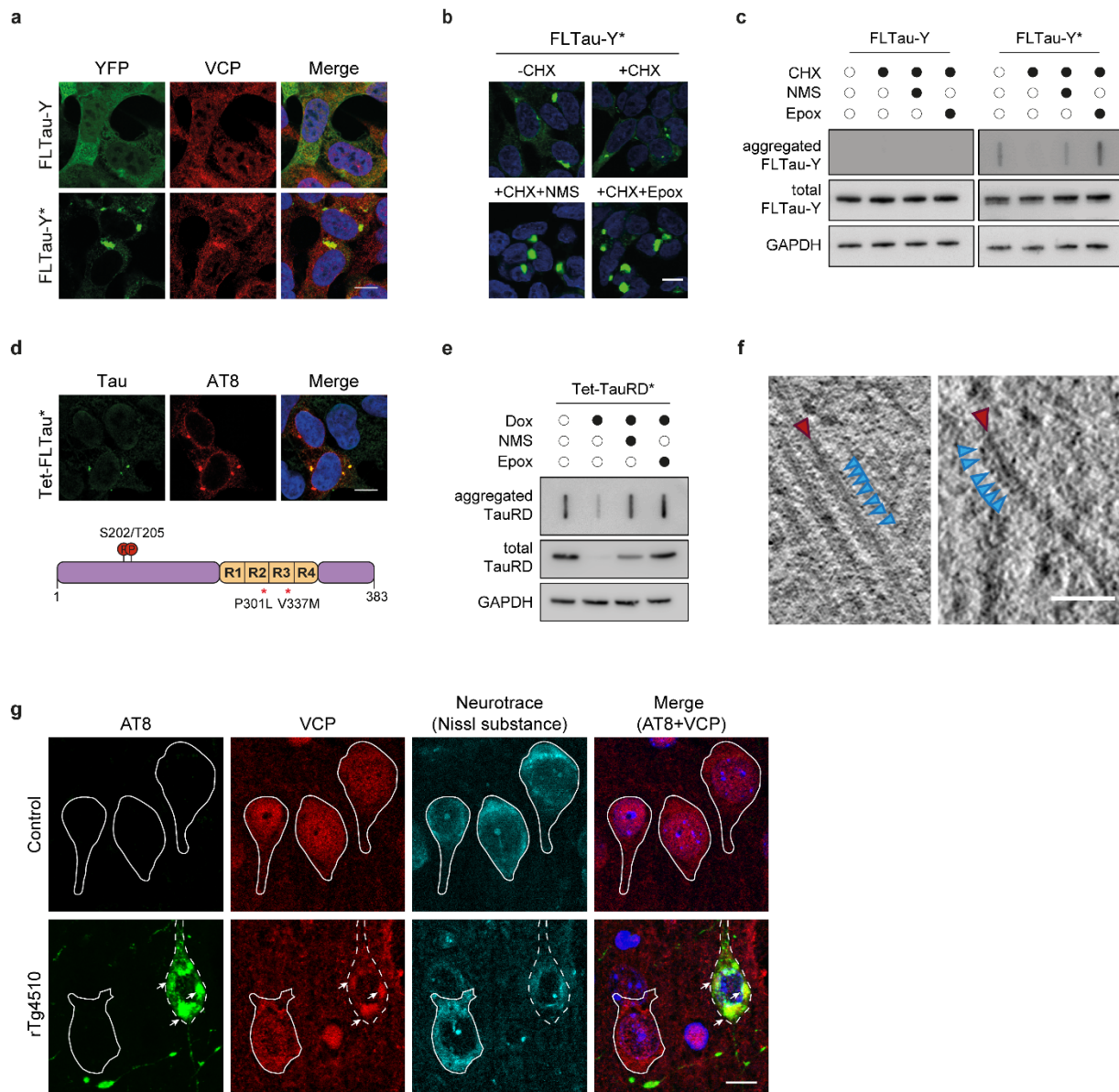
119 **Supplementary Fig. 5: Aggregation specific stabilization of Tau by VCP inactivation.**

120 **a** Immunofluorescence staining of VCP (red) and YFP fluorescence of TauRD-Y (green). **b** and **c**

121 Immunofluorescence staining of NPLOC4 (b) (red) and UFD1L (c) (red). Scale bars, 10 μm.

122 **d** Representative images of Tet-TauRD-Y\* cells treated with doxycycline (Dox; 50 ng/mL) alone

123 or in combination with CB-5083 (1  $\mu$ M) or NMS-873 (NMS; 2.5  $\mu$ M). Scale bar, 10  $\mu$ m. **e** Filter  
124 trap analysis of Tet-TauRD-Y\* cells treated as in (d). **f** Immunofluorescence staining of VCP (red)  
125 in Tet-TauRD-Y\* cells treated with non-targeted (Ctrl) or VCP siRNA for 96 h. Doxycycline  
126 (Dox; 50 ng/mL) was added for the last 24 h. Dashed lines indicate a cell with reduced VCP levels.  
127 Scale bar, 10  $\mu$ m. **g** Left, filter trap analysis of aggregated TauRD-Y in Tet-TauRD-Y\* lysates  
128 treated as in (f). Right, quantification of aggregated TauRD-Y. Mean  $\pm$  s.d.; n=3. \*p<0.05 (p=  
129 0.0174) from two-tailed Student's paired t-test. **h** Representative images of TauRD-Y\* cells  
130 treated with NMS-873 (NMS; 5  $\mu$ M) and quantification of average inclusion size ( $\mu$ m<sup>2</sup>). 200-400  
131 cells analyzed per experiment. Mean  $\pm$  s.d.; n=5. \*\*p<0.01 (p= 0.0022) from two-tailed Student's  
132 paired t-test. **i** Filter trap analysis of Tet-TauRD-Y cells treated with Epoxomicin (Epox; 50 nM)  
133 or NMS-873 (NMS; 2.5  $\mu$ M). Tet-TauRD-Y\* lysate was used as control. **j** Immunofluorescence  
134 staining of VCP (red) and YFP fluorescence of TauRD-Y (green) in Tet-TauRD-Y cells  
135 transfected with non-targeted (Ctrl) or VCP siRNA. Dashed lines indicate a cell with reduced VCP  
136 levels. Scale bar, 10  $\mu$ m. **k** Left, analysis of TauRD-Y level in Tet-TauRD-Y and Tet-TauRD-Y\*  
137 cells transfected for 96 h with non-targeted (Ctrl) or VCP siRNA. Doxycycline (Dox; 50 ng/mL)  
138 was added for the last 24 h. TauRD-Y was detected with anti-TauRD antibody. Right,  
139 quantification of TauRD-Y immunoblot. Mean  $\pm$  s.d.; n=4. \*p<0.05 (Tet-TauRD-Y - Dox: siCtrl  
140 vs siVCP, p= 0.0218; Tet-TauRD-Y\* + Dox: siCtrl vs siVCP, p= 0.0156); \*\*p<0.01 (Tet-TauRD-  
141 Y\* - Dox: siCtrl vs siVCP, p= 0.0023); n.s. non-significant (Tet-TauRD-Y + Dox: siCtrl vs siVCP,  
142 p= 0.0539) from two-tailed paired Student's t-test. Source data are provided as a Source Data file.



143

144 **Supplementary Fig. 6: Role of VCP in full length Tau disaggregation.**

145 **a** Immunofluorescence staining of VCP (red) and YFP fluorescence of FLTau-Y (green) in FLTau-

146 Y and FLTau-Y\* cells. Scale bar, 10  $\mu$ m. **b** Representative images of FLTau-Y\* cells treated for

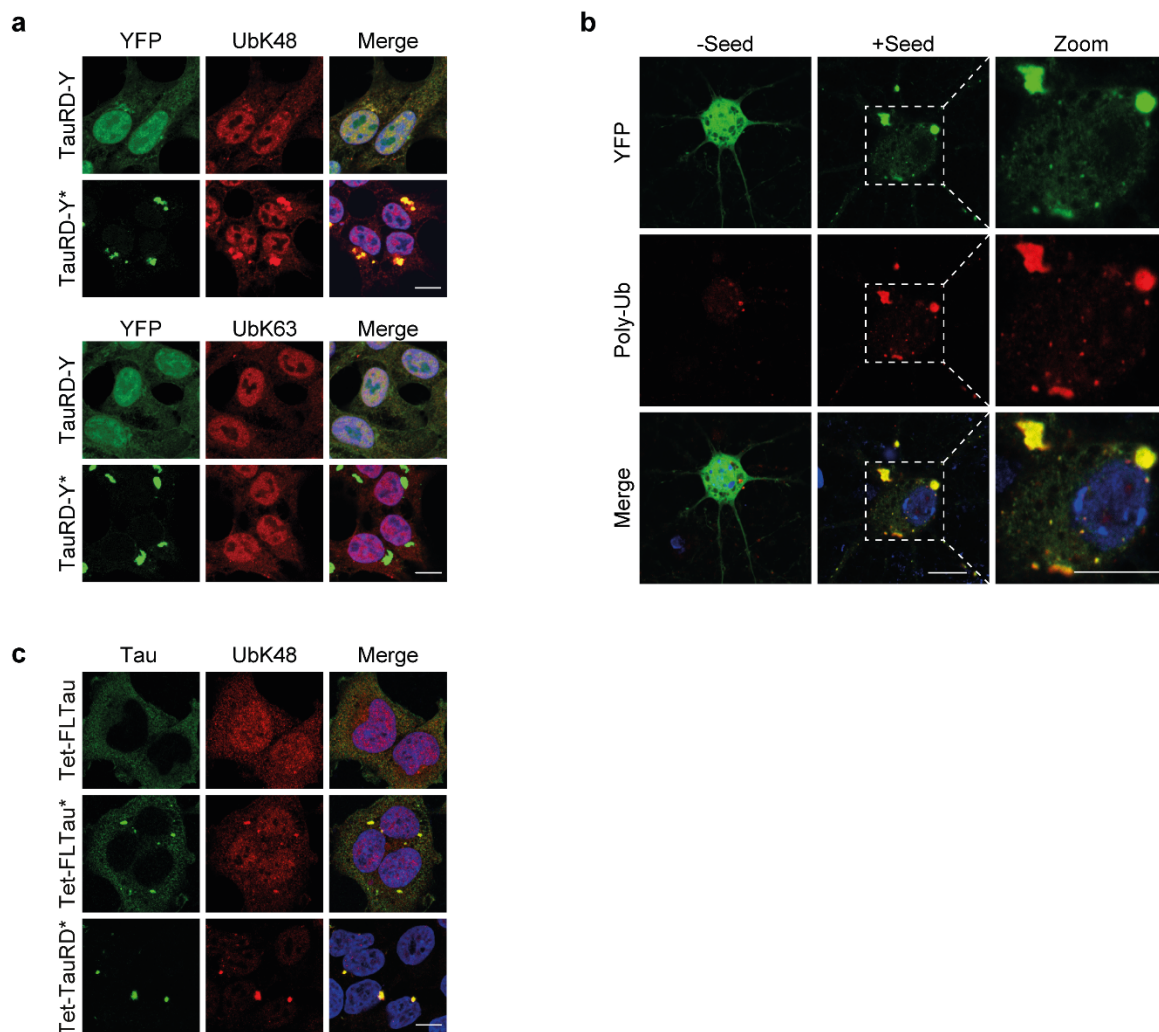
147 24 h with cycloheximide (CHX; 50  $\mu$ g/mL) alone or in combination with NMS-873 (NMS; 2.5

148  $\mu$ M) or Epoxomicin (Epox; 100 nM). Scale bar, 10  $\mu$ m. **c** Filter trap analysis of lysates from

149 FLTau-Y and FLTau-Y\* cells treated for 24 h with Dox alone or in combination with NMS-873

150 (NMS; 2.5  $\mu$ M) or Epoxomicin (Epox; 50 nM). Aggregated and total FLTau-Y levels were

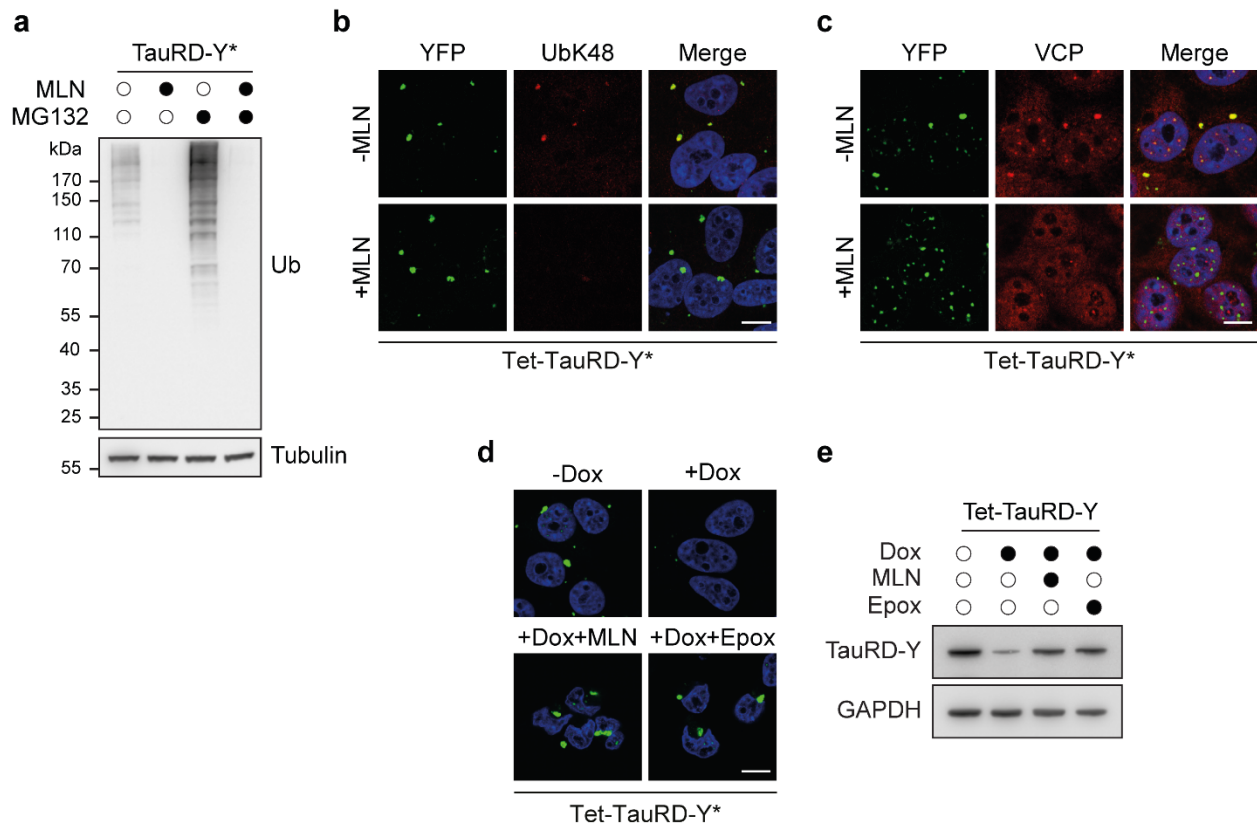
151 determined by immunoblotting against GFP. GAPDH served as loading control.  
152 **d** Immunofluorescence staining of full-length Tau (FLTau) in aggregate-containing Tet-FLTau\*  
153 cells with Tau (green) and Tau S202/T205 phosphorylation specific AT-8 (red) antibody. Scale  
154 bar, 10  $\mu$ m. **e** Filter trap analysis of lysates from Tet-TauRD\* cells treated for 24 h with Dox alone  
155 or in combination with NMS-873 (NMS; 2.5  $\mu$ M) or Epoxomicin (Epo; 50 nM). Aggregated and  
156 total TauRD levels were determined by immunoblotting against myc and TauRD, respectively.  
157 GAPDH served as loading control. **f** Examples of two TauRD-Y fibrils from a representative 1.4  
158 nm thick tomographic slice of a TauRD inclusion from neurons. Red arrowheads indicate TauRD-  
159 Y fibrils and blue arrowheads indicate globular densities along fibrils. Scale bar, 40 nm.  
160 **g** Immunofluorescence staining of brain sections of 4-month-old control and Tau transgenic  
161 rTg4510 mice with AT8 (green) and VCP (red) antibodies, Nissl substance (cyan) and DAPI (blue  
162 in the merged image). The outline of a cell containing phosphorylated Tau (p-Tau) is marked by a  
163 white dashed line. Cells not containing detectable p-Tau are marked by white continuous lines.  
164 Arrows point to VCP colocalizing with Tau inclusions. Scale bar, 10  $\mu$ m.  
165



166

167 **Supplementary Fig. 7: Ubiquitylation of TauRD-Y aggregates.**

168 **a** Immunofluorescence staining of (top) ubiquitin-K48 (UbK48) (red) and (bottom) ubiquitin K63  
 169 (UbK63) (red) chains and YFP fluorescence of TauRD-Y (green) in TauRD-Y and TauRD-Y\*  
 170 cells. Scale bars, 10  $\mu$ m. **b** Immunofluorescence staining of ubiquitylated proteins (FK2 antibody)  
 171 (red) in primary neurons expressing TauRD-Y (green) and treated with TauRD containing lysates  
 172 (+Seed) where indicated. Scale bars, 20  $\mu$ m. **c** Immunofluorescence staining of ubiquitin-K48  
 173 (UbK48) (red) chains and Tau (green) in Tet-FLTau, Tet-FLTau\* and Tet-TauRD\* cells. FLTau  
 174 was detected using Tau-5 and TauRD using anti-myc antibody. Scale bar, 10  $\mu$ m.

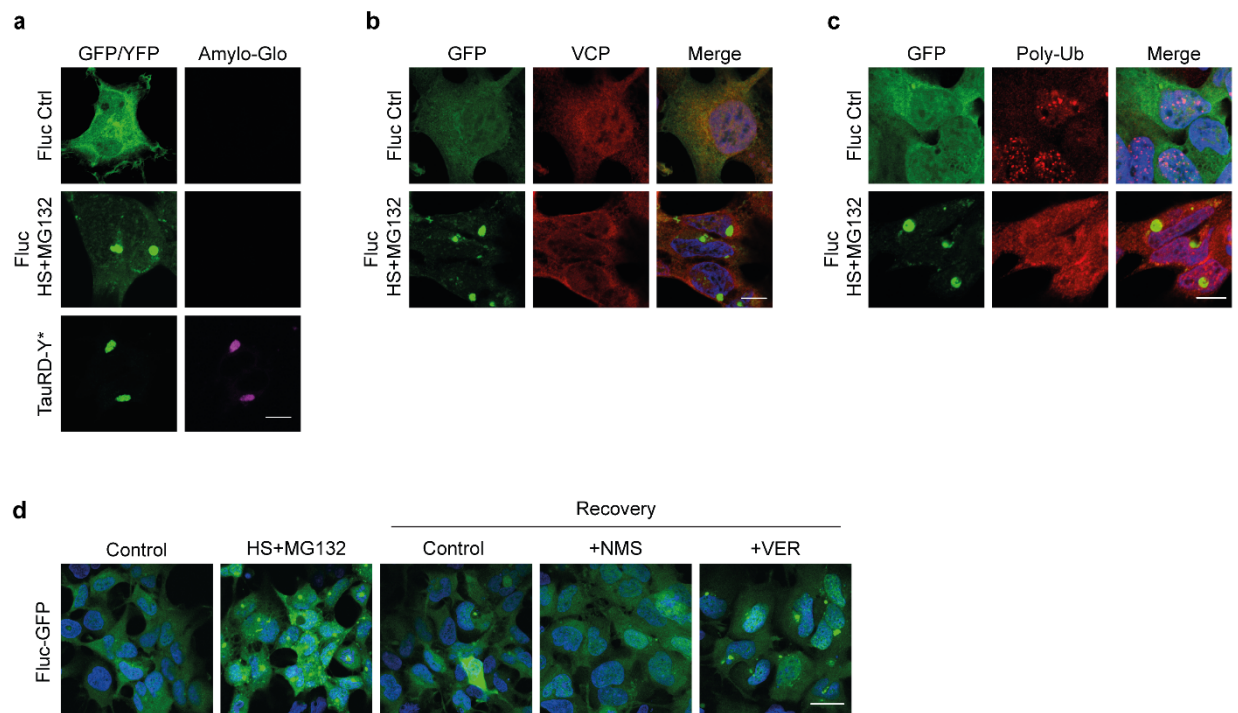


175

176 **Supplementary Fig. 8: Role of ubiquitylation in TauRD-Y disaggregation.**

177 **a** Analysis of ubiquitylated protein levels in lysates of TauRD-Y\* cells treated with the ubiquitin  
 178 activating enzyme E1 inhibitor MLN7243 (MLN; 0.5  $\mu$ M) alone or in combination with  
 179 proteasome inhibitor MG132 (1  $\mu$ M) for 14 h. Ubiquitylated proteins were detected by  
 180 immunoblotting against ubiquitin. Tubulin served as loading control. **b** Immunofluorescence  
 181 staining of ubiquitin-K48 chains (UbK48) (red) and **c** VCP (red) in Tet-TauRD-Y\* cells treated  
 182 with MLN7243 (MLN; 0.5  $\mu$ M) for 12 h. Scale bars, 10  $\mu$ m. **d** Representative images of Tet-  
 183 TauRD-Y\* cells treated for 24 h with doxycycline (Dox; 50 ng/mL) alone or in combination with  
 184 MLN7243 (MLN; 0.5  $\mu$ M) or Epoxomicin (Epox; 50 nM). Scale bar, 10  $\mu$ m. **e** Analysis of TauRD-  
 185 Y levels in Tet-TauRD-Y cells treated for 24 h with Dox, MLN7243 and Epoxomicin as in (d).  
 186 GAPDH served as loading control.

187

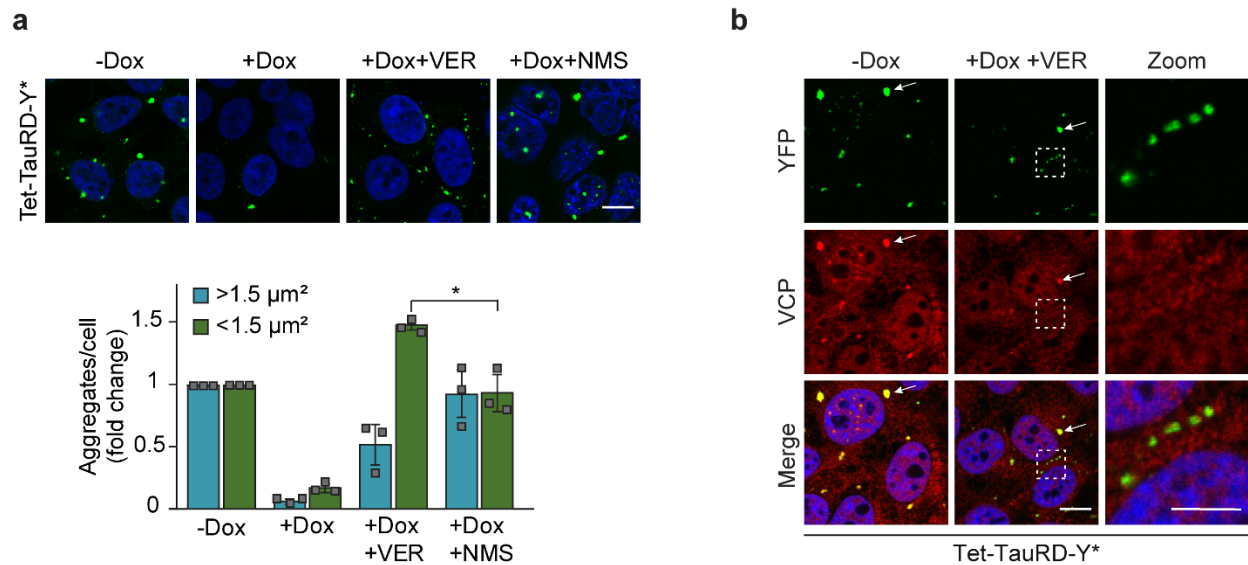


188

189 **Supplementary Fig. 9: Effect of VCP inhibition on firefly luciferase (Fluc) disaggregation.**

190 **a** Fluc-GFP expressing cells maintained at 37 °C (Fluc Ctrl) or heat-stressed at 43 °C in presence  
 191 of 5 μM MG132 for 2 h (Fluc HS) were stained with the amyloid-specific dye Amylo-Glo  
 192 (magenta). TauRD-Y\* cells were used as control. Amylo-Glo fluorescence was imaged with  
 193 similar exposure settings in all panels. Scale bar, 10 μm. **b** Immunofluorescence staining of VCP  
 194 (red), and **c** ubiquitylated proteins (FK2 antibody) (red) in Fluc-GFP cells treated as in (a). Scale  
 195 bars, 10 μm. **d** Effect of VCP and Hsp70 inhibition on Fluc-GFP disaggregation. Fluc-GFP  
 196 aggregation was induced as in (a). Cells were then shifted to MG132 free media and allowed to  
 197 recover at 37 °C for 8 h in presence of NMS-873 (NMS; 2.5 μM) and VER-155008 (VER; 10 μM)  
 198 where indicated. Scale bar, 30 μm.

199



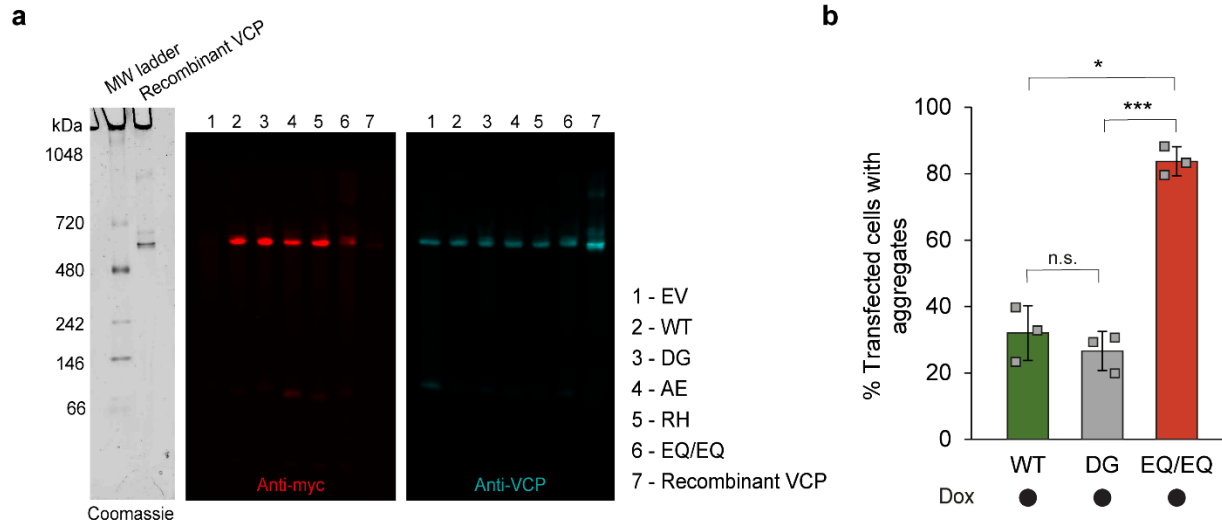
200

201 **Supplementary Fig. 10: Role of Hsp70 in TauRD-Y disaggregation.**

202 **a** Top, Representative images of Tet-TauRD-Y\* cells treated for 24 h with doxycycline (Dox; 50  
 203 ng/mL) alone or in combination with VER-155008 (VER; 10  $\mu\text{M}$ ) or NMS-873 (NMS; 2.5  $\mu\text{M}$ ).  
 204 Bottom, quantification of large (>1.5  $\mu\text{m}^2$ ) and small (<1.5  $\mu\text{m}^2$ ) TauRD-Y foci. Mean  $\pm$  s.d.; n=3;  
 205 ~100-200 cells were analyzed per experiment. \*p<0.05 (p=0.0435) from two-tailed Student's  
 206 paired t-test. Scale bar, 10  $\mu\text{m}$ . **b** Immunofluorescence staining of VCP (red) and YFP fluorescence  
 207 of TauRD-Y (green) in Tet-TauRD-Y\* cells treated with a combination of doxycycline (Dox) and  
 208 VER-155008 (VER) where indicated. White arrow points to large TauRD-Y inclusions co-  
 209 localizing with VCP. Dashed lines enclose TauRD-Y foci that do not co-localize with VCP. Scale  
 210 bar, 10  $\mu\text{m}$ . Scale bar zoom, 5  $\mu\text{m}$ . Source data are provided as a Source Data file.

211

212

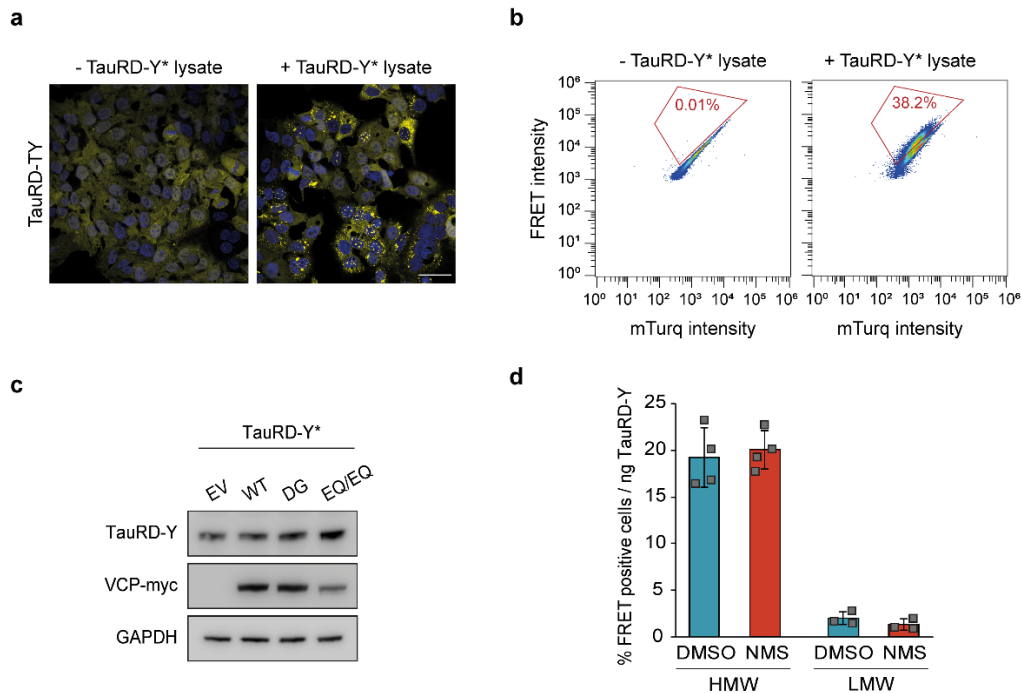


213  
214  
215

216 **Supplementary Fig. 11: Effect of VCP mutants on Tau disaggregation.**

217 **a** Native-PAGE analysis of recombinant VCP and lysates from Tet-TauRD-Y\* cells transfected  
218 with empty vector (EV) and myc-tagged wild type (WT), D395G (DG), A232E (AE), R155H (RH)  
219 and E305Q/E578Q (EQ/EQ) VCP constructs. Immunoblot probed against myc (red) and VCP  
220 (cyan) is shown. Non-tagged, recombinant VCP was analyzed as control. **b** Quantification of  
221 aggregate foci in myc-positive Tet-TauRD-Y\* cells transfected with myc-tagged WT, DG and  
222 EQ/EQ VCP constructs for 24 h, and treated for another 24 h with doxycycline (Dox; 50 ng/mL).  
223 Mean  $\pm$  s.d.; n=3; > 100 cells analyzed per experiment; \*p<0.05 (WT vs EQ/EQ p=0.0192);  
224 \*\*\*p<0.001 (DG vs EQ/EQ p=0.0008); n.s. non-significant (p=0.5646). Source data are provided  
225 as a Source Data file.

226

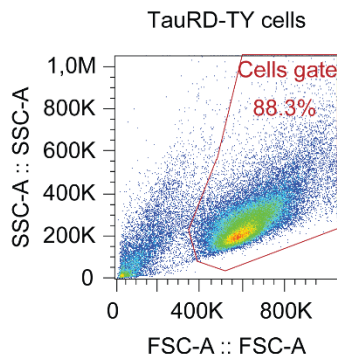


227

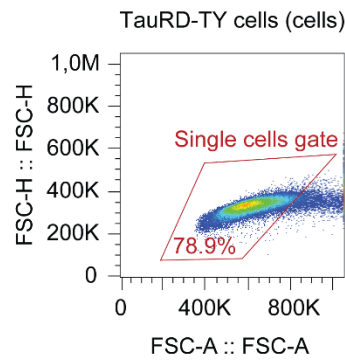
228 **Supplementary Fig. 12: Analysis of seeding-competent TauRD-Y.**

229 **a** Representative images of TauRD-TY FRET reporter cells treated with TauRD-Y\* lysate where  
 230 indicated showing TauRD-Y fluorescence in yellow. Scale bar, 40  $\mu$ m. **b** Representative  
 231 pseudocolour dot plots for the analysis of FRET positive TauRD-TY cells by flow cytometry upon  
 232 addition of TauRD-Y\* lysate. FRET intensity is plotted against mTurquoise2 (mTurq) intensity  
 233 and the % of FRET positive cells are indicated in red gates. **c** Analysis of TauRD-Y and VCP-myc  
 234 levels in TauRD-Y\* cells transfected for two days with empty vector (EV) and myc-tagged wild  
 235 type (WT), D395G (DG) and E305Q/E578Q (EQ/EQ) VCP constructs. TauRD-Y and  
 236 overexpressed VCP levels were determined by immunoblotting against GFP and myc,  
 237 respectively. GAPDH served as loading control. **d** Comparison of seeding efficiencies of high  
 238 molecular weight (HMW) and low molecular weight (LMW) species obtained by size exclusion  
 239 chromatography of lysates from TauRD-Y\* cells treated for 24 h with DMSO or NMS-873 (NMS;  
 240 2  $\mu$ M). Mean  $\pm$  s.d.; HMW n=4, LMW n=3. Source data are provided as a Source Data file.

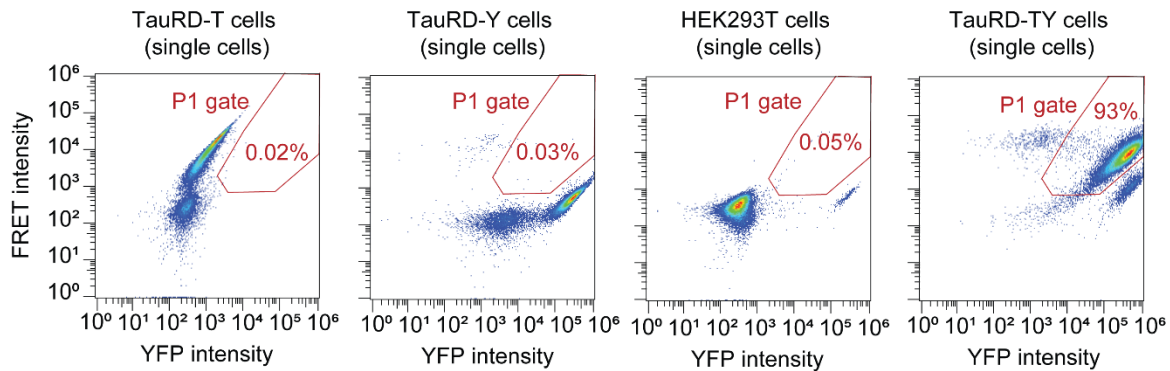
### 1. Selection of cells



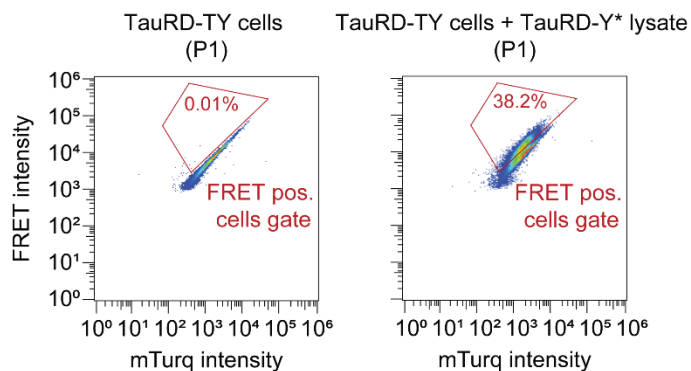
### 2. Selection of single cells



### 3. Exclusion of possible false positive FRET signal resulting from YFP excitation by the 405 nm laser (exclusion from P1 gate)<sup>1</sup>



### 4. Selection of FRET positive cells from the P1 population using non-seeded cells as reference



241 **Supplementary Fig. 13: Flow cytometry strategy for quantification of FRET positive cells.**

242 To measure the mTurquoise2 and FRET fluorescence signals, cells were excited with 405 nm laser

243 light and fluorescence was determined using 440/50 and 530/30 filters, respectively. To measure

244 the YFP fluorescence signal, cells were excited at 488 nm and emission was recorded using a

245 530/30 filter. For each sample, 50,000 single cells were analyzed, using a gating strategy recently  
246 described<sup>1,2</sup>. First, cells were selected (1), followed by single cell selection (2). After gating single  
247 cells, an additional gate (P1) was introduced to exclude YFP-only cells that show a false-positive  
248 signal in the FRET channel due to excitation at 405 nm using TauRD-T cells, TauRD-Y cells and  
249 HEK293T cells<sup>1,2</sup> as reference (3). The FRET positive gate was set by plotting the FRET  
250 fluorescence signal versus the mTurquoise2 fluorescence signal using non-seeded cells as  
251 reference (4). Note that some panels in (1)-(3) were recently published describing the gating  
252 strategy for a comparable experiment<sup>2</sup>.

253

#### 254 **Supplementary references**

- 255 1 Banning, C. *et al.* A flow cytometry-based FRET assay to identify and analyse protein-  
256 protein interactions in living cells. *PLoS One* **5**, e9344 (2010).
- 257 2 Yuste-Checa, P. *et al.* The extracellular chaperone Clusterin enhances Tau aggregate  
258 seeding in a cellular model. *Nature Communications* **12**, 4863 (2021).

259 **Supplementary Table 1. TauRD-Y interactome in TauRD-Y\* cells**

260 List of proteins interacting with TauRD-Y in TauRD-Y\* cells at steady state determined by stable isotope labelling by amino acids in cell  
 261 culture (SILAC). TauRD-Y cells were used as control. Normalized SILAC ratios of TauRD-Y\*/TauRD-Y [H/L] from 3 independent  
 262 replicates are shown. Interactors were defined as proteins quantified in at least 2 out of 3 replicates with enrichment  $\geq 2$  fold. Proteins with  
 263 known association to the ubiquitin-proteasome system are highlighted in green and VCP-cofactor complex in red. Intensity-based absolute  
 264 quantification (iBAQ) values reflect measured molar protein amounts.

Protein ID	Protein name	Gene name	Fasta headers	Unique peptides	Mol. weight [kDa]	Norm. ratio [H/L] Rep.1	Norm. ratio [H/L] Rep.2	Norm. ratio [H/L] Rep.3	Median norm. ratio	iBAQ [H] Exp.1	iBAQ [H] Exp.2	iBAQ [H] Exp.3
Q9UNZ2;FZ	NSFL1 cofactor p47	NSFL1C	sp Q9UNZ2 NSF1C_HUMAN NSFL1 cofactor p47 OS=	14	40.572	42.702	80.022	11.719	42.702	59143000	112180000	13783000
Q9UQN3;AC	Charged multivesicular body protein 2b	CHMP2B	sp Q9UQN3 CHM2B_HUMAN Charged multivesicu	4	23.906	18.201	25.514	11.839	18.201	2093000	5417800	15472000
P55072;C9I2	Transitional endoplasmic reticulum ATPase	VCP	sp P55072 TERA_HUMAN Transitional endoplasmii	47	89.321	16.959	43.344	6.3181	16.959	29193000	94165000	26411000
Q9UNM6;J3	26S proteasome non-ATPase regulatory sub	PSMD13	sp Q9UNM6 PSD13_HUMAN 26S proteasome non-A	22	42.945	17.963	16.071	13.583	16.071	9313200	17290000	5085700
Q6PEV8	Protein FAM199X	FAM199X	sp Q6PEV8 F199X_HUMAN Protein FAM199X OS=H	5	42.801	41.449	15.154	15.115	15.154	9838300	30031000	10267000
F8VUA2;Q9	Charged multivesicular body protein 1a	CHMP1A	tr F8VUA2 F8VUA2_HUMAN Charged multivesicula	5	19.531	14.648	19.186	12.293	14.648	25912000	113020000	38592000
Q15773;F5H	Myeloid leukemia factor 2	MLF2	sp Q15773 MLF2_HUMAN Myeloid leukemia factor	6	28.147	16.867	13.819	6.564	13.819	74907000	153440000	42871000
O43242;H0Y	26S proteasome non-ATPase regulatory sub	PSMD3	sp O43242 PSMD3_HUMAN 26S proteasome non-A	34	60.977	13.413	15.879	6.9978	13.413	21734000	50167000	10257000
O00231;J3Q	26S proteasome non-ATPase regulatory sub	PSMD11	sp O00231 PSD11_HUMAN 26S proteasome non-A	26	47.463	13.086	22.385	7.5615	13.086	14133000	35102000	7362100
P62191;G3V	26S protease regulatory subunit 4	PSMC1	sp P62191 PRS4_HUMAN 26S proteasome regulat	20	49.184	12.739	13.685	6.7346	12.739	6082800	18968000	4723500
P17480	Nucleolar transcription factor 1	UBTF	sp P17480 UBF1_HUMAN Nucleolar transcription f	22	89.405	12.209	11.585	7.1602	11.585	94071000	144030000	43389000
O14545;F8V	TRAF-type zinc finger domain-containing pr	TRAFD1	sp O14545 TRAD1_HUMAN TRAF-type zinc finger c	12	64.84	7.2319	19.2	11.522	11.522	6914300	16022000	16301000
Q13501;E7E	Sequestosome-1	SQSTM1	sp Q13501 SQSTM1_HUMAN Sequestosome-1 OS=H	16	47.687	9.6152	17.975	11.41	11.41	27933000	113830000	115270000
Q13200;C9I	26S proteasome non-ATPase regulatory sub	PSMD2	sp Q13200 PSMD2_HUMAN 26S proteasome non-A	46	100.2	7.2067	22.927	11.267	11.267	4555900	9942100	6380700
H0Y6K2;A04	Bromodomain-containing protein 2	BRD2	tr H0Y6K2 H0Y6K2_HUMAN Bromodomain-contain	11	88.288	24.922	7.6855	10.958	10.958	6685300	16169000	6613700
H0YFD6;P4C	Trifunctional enzyme subunit alpha, mitoch	HADHA	tr H0YFD6 H0YFD6_HUMAN Trifunctional enzyme s	29	86.371	10.902	11.422	8.175	10.902	45516000	92103000	31426000
P55036;Q5V	26S proteasome non-ATPase regulatory sub	PSMD4	sp P55036 PSMD4_HUMAN 26S proteasome non-A	14	40.736	12.228	10.9	3.7986	10.9	19080000	82099000	8516700
Q6QNY1;J3K	Biogenesis of lysosome-related organelles	BLOC1S2	sp Q6QNY1 BL1S2_HUMAN Biogenesis of lysosom	3	15.961	10.78	15.848	2.0051	10.78	1892700	3652000	1718300
P55084;F5G	Trifunctional enzyme subunit beta, mitochc	HADHB	sp P55084 ECHB_HUMAN Trifunctional enzyme sul	25	51.294	9.9693	11.079	8.0079	9.9693	65103000	128900000	39724000
P25788;G3V	Proteasome subunit alpha type-3	PSMA3	sp P25788 PSA3_HUMAN Proteasome subunit alp	9	28.433	3.0605	14.754	9.9671	9.9671	2846500	1743900	2866700
A8MUA9;A6	Small ubiquitin-related modifier 4;Small ub	SUMO3;SUM	tr A8MUA9 A8MUA9_HUMAN SMT3 suppressor of	1	15.317	8.4377	11.126		9.78185	14432000	26087000	0
Q8TAT6;J3L	Nuclear protein localization protein 4 homo	NPLOC4	sp Q8TAT6 NPL4_HUMAN Nuclear protein localiza	17	68.119	3.9291	15.451		9.69005	1208400	5604000	0
P25789;H0Y	Proteasome subunit alpha type-4;Proteasor	PSMA4	sp P25789 PSA4_HUMAN Proteasome subunit alp	10	29.483	2.7706		16.307	9.5388	4339400	0	4387000
Q9UHD9	Ubiquilin-2	UBQLN2	sp Q9UHD9 UBQL2_HUMAN Ubiquilin-2 OS=Homo	11	65.695	6.6843	11.794		9.23915	8201000	24600000	108990
O14818;H0V	Proteasome subunit alpha type-7	PSMA7	sp O14818 PSA7_HUMAN Proteasome subunit alp	14	27.887	2.6045	9.1585	10.57	9.1585	3845500	10551000	10021000
Q9UID3;E9F	Vacuolar protein sorting-associated protein	VPS51	sp Q9UID3 VPS51_HUMAN Vacuolar protein sortin	11	86.041	12.8	5.2875		9.04375	603160	3513600	552200
Q14596;B7Z	Next to BRCA1 gene 1 protein	NBR1	sp Q14596 NBR1_HUMAN Next to BRCA1 gene 1 pr	12	107.41	15.113		2.4528	8.7829	0	12693000	12934000
Q92890;C9I	Ubiquitin fusion degradation protein 1 hom	UFD1L	sp Q92890 UFD1_HUMAN Ubiquitin recognition fa	9	34.5	11.411	6.134		8.7725	785590	5835400	721170
Q15008;C9I	26S proteasome non-ATPase regulatory sub	PSMD6	sp Q15008 PSMD6_HUMAN 26S proteasome non-A	27	45.531	7.3639	9.6008		8.555	13494000	32338000	6986900

265  
266

Continued on next page

Protein ID	Protein name	Gene name	Fasta headers	Unique peptides	Mol. weight [kDa]	Norm. ratio [H/L]	Rep.1	Norm. ratio [H/L]	Rep.2	Norm. ratio [H/L]	Rep.3	Median norm. ratio	iBAQ [H] Exp.1	iBAQ [H] Exp.2	iBAQ [H] Exp.3	
Q96DX7	Tripartite motif-containing protein 44	TRIM44	sp Q96DX7 TRIM44_HUMAN Tripartite motif-contain	5	38.472	10.369		6.5983				8.48365	708170	19187000	783500	
Q16643;D6f	Drebrin	DBN1	sp Q16643 DREB_HUMAN Drebrin OS=Homo sapie	16	71.428			13.93		2.7427		8.33635	123350	13631000	6342500	
A0A087X211	26S protease regulatory subunit 10B	PSMG6	tr A0A087X211 A0A087X211_HUMAN 26S proteasor	16	45.796	10.533		6.0398				8.2864	2266900	10434000	743130	
P51665;H3B	26S proteasome non-ATPase regulatory sub	PSMD7	sp P51665 PSMD7_HUMAN 26S proteasome non-A	14	37.025	8.2466		13.713		6.6956		8.2466	9133800	34517000	6064400	
P35998;A0A	26S protease regulatory subunit 7	PSMC2	sp P35998 PR57_HUMAN 26S proteasome regulat	24	48.633	7.5017		8.0742				8.5178	8531200	12549000	5021100	
B3KVL5;Q8I	Zinc finger CCHC domain-containing protein	ZCCHC10	tr B3KVL5 B3KVL5_HUMAN Zinc finger, CCHC domi	1	20.308			7.1775		8.4956		7.83655	18527000	60508000	11466000	
Q8IXW5	Putative RNA polymerase II subunit B1 CTD	RPAP2	sp Q8IXW5 RPAP2_HUMAN Putative RNA polymer	13	69.508	10.475		7.8181		3.3996		7.8181	1205400	8566200	4524400	
P62979;J3Q	Ubiquitin-40S ribosomal protein S27a;Ubiqu	RPS27A;UBB1	sp P62979 RS27A_HUMAN Ubiquitin-40S ribosoma	10	17.965	9.4683		7.6945		4.1911		7.6945	3164100000	7019100000	1951400000	
Q99460;A0A	26S proteasome non-ATPase regulatory sub	PSMD1	sp Q99460 PSMD1_HUMAN 26S proteasome non-A	42	105.84	6.684		7.415		7.8358		7.415	3058500	12531000	2851500	
P43686	26S protease regulatory subunit 6B	PSMC4	sp P43686 PR56B_HUMAN 26S proteasome regul	21	47.366	8.4576		2.5541		6.7907		6.7907	1137200	10458000	617140	
R4GMRS;K7	26S proteasome non-ATPase regulatory sub	PSMD8	tr R4GMRS R4GMRS_HUMAN 26S proteasome non	10	32.551	1.3779		6.6145		13.37		6.6145	491820	3751000	6211100	
POCAP2;H8	DNA-directed RNA polymerase II subunit Gf	POLR2M;GCC	sp POCAP2 GRL1A_HUMAN DNA-directed RNA pol	4	41.739	6.9552		6.1579				6.55655	2999600	6478700	0	
P49721;A0A	Proteasome subunit beta type-2	PSMB2	sp P49721 PSB2_HUMAN Proteasome subunit beta	10	22.836	2.6138		10.075				6.3444	526870	3115400	1949400	
Q9UQ35;J3L	Serine/arginine repetitive matrix protein 2	SRRM2	sp Q9UQ35 SRRM2_HUMAN Serine/arginine repet	44	299.61	8.8182		4.1061		6.3418		6.3418	40059000	69443000	34477000	
O75487	Glypican-4;Secreted glypican-4	GPC4	sp O75487 GPC4_HUMAN Glypican-4 OS=Homo sa	13	62.411	6.1176		9.697				6.1176	1230600	31449000	4359700	
Q9H307;G3P	Pinin	PNIN	sp Q9H307 PININ_HUMAN Pinin OS=Homo sapien	39	81.627	6.4613		5.9829				5.9829	180190000	359840000	205880000	
Q99615;K7E	DnaJ homolog subfamily C member 7	DNAJC7	sp Q99615 DNJC7_HUMAN DnaJ homolog subfami	35	56.44	32.017		5.9433				3.8506	58381000	56886000	13723000	
O95816	BAG family molecular chaperone regulator	BAG2	sp O95816 BAG2_HUMAN BAG family molecular ch	9	23.772	5.7371		8.5666				3.8905	5.7371	10758000	36658000	8833600
Q9BYN8	28S ribosomal protein S26, mitochondrial	MRPS26	sp Q9BYN8 RT26_HUMAN 28S ribosomal protein S	7	24.211	5.6963		5.8954				3.1697	5.6963	5578000	11868000	
P10644;K7E	cAMP-dependent protein kinase type I- $\alpha$	PRKAR1A	sp P10644 KAP0_HUMAN cAMP-dependent protei	12	42.981	5.6698		8.1797				2.4289	5.6698	1804900	8873600	3456600
A0A0C4DG6	ADP-ribosylation factor-like protein 6-inter	ARL6IP4	tr A0A0C4DG6 A0A0C4DG62_HUMAN ADP-ribosy	5	24.591	6.5334		5.8168		2.4357		5.6534	11791000	37307000	7853000	
Q15545	Transcription initiation factor TFIID subunit	TAF7	sp Q15545 TAF7_HUMAN Transcription initiation f	5	40.259	6.7383		4.5475				5.6429	1917000	3824800	262590	
F5H442;Q9S	Tumor susceptibility gene 101 protein	TSG101	tr F5H442 F5H442_HUMAN Tumor susceptibility ge	8	40.917	6.9756		3.423				5.1993	1298100	2512100	0	
Q14677;H0N	Clathrin interactor 1	CUN11	sp Q14677 EPN4_HUMAN Clathrin interactor 1 OS=	17	68.259	4.5671		5.1051				4.8361	483270	1390800	0	
Q16531;F5C	DNA damage-binding protein 1	DDB1	sp Q16531 DDB1_HUMAN DNA damage-binding pr	51	126.97	5.1552		4.8124		4.7395		4.8124	2260500	20150000	818320	
Q14646;H0N	Chromodomain-helicase-DNA-binding protein	CHD1	sp Q14646 CHD1_HUMAN Chromodomain-helicasi	22	196.69	4.667		5.6909				4.667	1212300	6836700	855680	
G3V5Z7;P6G	Proteasome subunit alpha type;Proteasome	PSMA6	tr G3V5Z7 G3V5Z7_HUMAN Proteasome subunit a	12	28.147			5.4361				3.7845	0	986560	3211200	
P17980;E9P	26S protease regulatory subunit 6A	PSMC3	sp P17980 PR56A_HUMAN 26S proteasome regula	21	49.203	5.2382		3.8803				4.55925	2297800	7983700	563940	
O00232;J3K	26S proteasome non-ATPase regulatory sub	PSMD12	sp O00232 PSD12_HUMAN 26S proteasome non-A	22	52.904	4.4642		2.2919		13.215		4.4642	5157500	5534500	3641700	
P61964;Y9C	WD repeat-containing protein 5	WDR5	sp P61964 WDR5_HUMAN WD repeat-containing p	5	36.588	2.7665		5.5202				4.14335	1116200	6218500	163100	
O00487;C9J	26S proteasome non-ATPase regulatory sub	PSMD14	sp O00487 PSDE_HUMAN 26S proteasome non-AT	10	34.577	4.4008		3.6454				4.0231	2763600	4175800	1273000	
P62195;J3Q	26S protease regulatory subunit 8	PSMC5	sp P62195 PR58_HUMAN 26S proteasome regulat	23	45.626	4.5333		4.0178		2.4837		4.0178	2401900	10162000	3258800	
P24928	DNA-directed RNA polymerase II subunit RF	POLR2A	sp P24928 RPB1_HUMAN DNA-directed RNA polyr	51	217.17	3.9675		4.1625		3.3865		3.9675	5036400	22719000	4400000	
O14974;F8V	Protein phosphatase 1 regulatory subunit 1	PPP1R12A	sp O14974 MYPT1_HUMAN Protein phosphatase 1	15	115.28	3.6323		4.1458				3.88905	135210	738040	0	
Q5VIR6;F6V	Vacuolar protein sorting-associated protein	VP53	sp Q5VIR6 VP53_HUMAN Vacuolar protein sortin	10	79.652			2.3872				5.2434	0	867750	158630	
Q8WV44;H	E3 ubiquitin-protein ligase TRIM41	TRIM41	sp Q8WV44 TRIM41_HUMAN E3 ubiquitin-protein li	5	71.669	4.3208		3.4885				3.7734	613000	252640	1261800	
F8W118;F8V	59;B729C2;F8VRJ2	NAP1L1	tr F8W118 F8W118_HUMAN Nucleosome assembl	12	24.694	3.6447		4.8952				3.6447	4807500	20158000	2227100	
E9PNW4;A	CD59 glycoprotein	CD59	tr E9PNW4 E9PNW4_HUMAN Uncharacterized pro	4	11.985			4.7462				2.1357	3.44095	5131200	54954000	35045000
Q96BQ5	Coiled-coil domain-containing protein 127	CCDC127	sp Q96BQ5 CC127_HUMAN Coiled-coil domain-coi	4	30.834	4.0401						2.7807	3.4104	3768100	3178900	697410
O43164	E3 ubiquitin-protein ligase Praja-2	PJA2	sp O43164 PJA2_HUMAN E3 ubiquitin-protein liga	15	78.213	3.3397		6.1296				3.3397	4791500	29710000	8235700	
B8ZD4;Q8T	Tax1-binding protein 1	TAX1BP1	tr B8ZD4 B8ZD4_HUMAN Tax1-binding protein 1	14	93.609	9.5213		3.2831				3.1608	409770	4896800	4112000	
P62857	40S ribosomal protein S28	RPS28	sp P62857 RS28_HUMAN 40S ribosomal protein S2	2	7.8409	3.7217		3.2677				1.1842	18987000	32783000	6557100	
P62873;F6U	Guanine nucleotide-binding protein G(i)/G	(GNB1)	sp P62873 GBB1_HUMAN Guanine nucleotide-bind	13	37.377	3.2364		4.2746				1.6165	3.2364	2812200	17175000	35389000
Q7L7X3;J3Q	Serine/threonine-protein kinase TAO1	TAOK1	sp Q7L7X3 TAOK1_HUMAN Serine/threonine-prot	15	116.07	1.3856		3.2072				3.0804	2889600	6633200	6110200	
O75955;A0F	Flotillin-1	FLOT1	sp O75955 FLOT1_HUMAN Flotillin-1 OS=Homo sa	16	47.355	3.0802		3.6951				1.7534	3.0802	11366000	21730000	4780700
Q12899;A2J	Tripartite motif-containing protein 26	TRIM26	sp Q12899 TRI26_HUMAN Tripartite motif-contain	7	62.165	4.126		2.001				3.0635	1519900	2525100	1427900	
O99986;H0N	Serine/threonine-protein kinase VRK1	VRK1	sp O99986 VRK1_HUMAN Serine/threonine-prot	14	45.476	3.4612		3.0568				3.0568	2738700	26700000	18471000	
C9J2Y9;P30I	DNA-directed RNA polymerase;DNA-direct	POLR2B	tr C9J2Y9 C9J2Y9_HUMAN DNA-directed RNA poly	34	133.06	3.7497		3.0177				3.0513	4282800	9848300	392790	
H3BV80;H3I	RNA-binding protein with serine-rich doma	RNPS1	tr H3BV80 H3BV80_HUMAN RNA-binding protein	6	24.561	3.0441		3.3076				2.5543	139510000	204410000	94293000	
Q9UBI6	Guanine nucleotide-binding protein G(i)/G	(GNL1)	sp Q9UBI6 GBG12_HUMAN Guanine nucleotide-bi	3	8.0061	3.0438		4.9367				2.0117	3890300	34430000	84342000	

267

268

Continued on next page

Protein ID	Protein name	Gene name	Fasta headers	Unique peptides	Mol. weight [kDa]	Norm. ratio [H/L]	Rep.1	Norm. ratio [H/L]	Rep.2	Norm. ratio [H/L]	Rep.3	Median norm. ratio	lBAQ [H] Exp.1	lBAQ [H] Exp.2	lBAQ [H] Exp.3	
I1E4Y6;QGY	PERQ amino acid-rich with GYF domain-cont	GIGYF2	tr I1E4Y6 I1E4Y6_HUMAN GRB10-interacting GYF pi	11	152.53	3.4506		2.6293				3.03995	571610	1017200	0	
P16403;P10	Histone H1.2;Histone H1.4	HIST1H1C;HIS	sp P16403 H12_HUMAN Histone H1.2 OS=Homo sa	12	21.364	3.0264		2.2983		3.593		3.0264	103310000	303900000	129810000	
P19387;H3B	DNA-directed RNA polymerase II subunit RF	POLR2C	sp P19387 RPB3_HUMAN DNA-directed RNA polyr	10	31.441	3.0233		3.8035		2.6379		3.0233	11207000	18173000	2879500	
Q5HYB6	Chromatin assembly factor 1 subunit B	CHAF1B	tr Q5HYB6 Q5HYB6_HUMAN Epididymis luminal pr	21	27.175	4.5555		2.9635		2.9779		2.9779	1471400	6297900	1443000	
P06748;E5R	Nucleophosmin	NPM1	sp P06748 NPM1_HUMAN Nucleophosmin OS=Homo	17	32.575	3.5369		2.9192		1.7384		2.9192	45741000	124660000	102380000	
J3QLD9;E7E	Flotillin-2	FLOT2	tr J3QLD9 J3QLD9_HUMAN Flotillin-2 OS=Homo sa	15	47.142	2.9067		4.1686		1.6969		2.9067	8440000	26271000	11510000	
P62879;C9J	Guanine nucleotide-binding protein G(i)/G	GNB2	sp P62879 G8B2_HUMAN Guanine nucleotide-bin	12	37.331	2.9058		4.836		1.5201		2.9058	4881400	14551000	15388000	
Q53H12;E9F	Acylglycerol kinase, mitochondrial	AGK	sp Q53H12 AGK_HUMAN Acylglycerol kinase, mitc	18	47.137	1.1258		2.8627		4.0535		2.8627	4820100	15152000	13972000	
Q13112	Chromatin assembly factor 1 subunit B	CHAF1B	sp Q13112 CAF1B_HUMAN Chromatin assembly fa	4	61.492	2.844		2.8809				2.86245	512590	77757	0	
A0A087WV7	DNA-directed RNA polymerases I, II, and III	POLR2E	tr A0A087WVZ9 A0A087WVZ9_HUMAN DNA-direc	7	21.459	3.1167		2.4935				2.8051	3322300	15849000	0	
Q92820	Gamma-glutamyl hydrolase	GGH	sp Q92820 GGH_HUMAN Gamma-glutamyl hydroly	8	35.964	2.8025		5.1253		2.0979		2.8025	2133200	7381800	1489700	
Q96GA3;A0	Protein LTV1 homolog	LTV1	sp Q96GA3 LTV1_HUMAN Protein LTV1 homolog C	15	54.854	1.3874		3.0356		2.7805		2.7805	11848000	15414000	11793000	
P60709;A0A	Actin, cytoplasmic 1;Actin, cytoplasmic 1, N-ACTB	ACTB	sp P60709 ACTB_HUMAN Actin, cytoplasmic 1 OS=	27	41.736	1.2178		3.5005		2.7751		2.7751	11323000	36019000	20782000	
Adde01;CON	_Q9U6Y5;I3L170		tr Adde01 TauYfp_HUMAN Tau Yfp	39	43.256	3.5063		2.7256				2.7256	4130100000	891400000	3833400000	
Q99613;B5A	Eukaryotic translation initiation factor 3 sub	EIF3C;EIF3CL	sp Q99613 EIF3C_HUMAN Eukaryotic translation ir	33	105.34	2.5577		2.8357				2.6967	855670	4670000	443520	
P28066	Proteasome subunit alpha type-5	PSMA5	sp P28066 PSA5_HUMAN Proteasome subunit alpi	13	26.411	3.108		3.108		2.254		2.681	713200	3627100	526020	
Q9HCM4	Band 4.1-like protein 5	EPB41L5	sp Q9HCM4 E41L5_HUMAN Band 4.1-like protein 5	9	81.855	2.1785		3.0182				2.59835	227100	3722200	0	
A0A087WVY	Slit homolog 2 protein;Slit homolog 2 prote	SLIT2	tr A0A087WVY5 A0A087WVY5_HUMAN Slit homol	9	159.98	2.0219		3.1071				2.5645	487410	1400300	599630	
A0A1W2PQ	DNA repair protein RAD50	RAD50	tr A0A1W2PQ90 A0A1W2PQ90_HUMAN Uncharact	25	142.94	2.5131		3.214		0.89296		2.5131	5120600	5250600	1514700	
Q9H0U4;E9I	Ras-related protein Rab-1B;Putative Ras-re	RAB1B;RAB1B1	sp Q9H0U4 RAB1B_HUMAN Ras-related protein R	12	22.171	2.7446		2.7446				2.1603	2.45245	682330	3902100	564680
Q13823;H0N	Nucleolar GTP-binding protein 2	GNL2	sp Q13823 NOG2_HUMAN Nucleolar GTP-binding	18	83.654	2.5228		2.3703				2.44655	504360	3938100	57885	
Q07021;I3L	Complement component 1 Q subcomponent	C1QBP	sp Q07021 C1QBP_HUMAN Complement compone	10	31.362	2.1285		5.1114		2.4395		2.4395	5133600	39902000	12700000	
Q72417	Nuclear fragile X mental retardation-interac	NUFIP2	sp Q72417 NUFP2_HUMAN Nuclear fragile X ment	15	76.12	2.9962		2.4364		2.0328		2.4364	5829600	7837800	5467700	
P08670;B0Y	Vimentin	VIM	sp P08670 VIME_HUMAN Vimentin OS=Homo sapi	45	55.651	2.4027		2.6728		1.6894		2.4027	59024000	131930000	146780000	
P19525;C9J	Interferon-induced, double-stranded RNA-;	EIF2AK2	sp P19525 E2AK2_HUMAN Interferon-induced, do	12	62.094	2.5648		2.384		2.0421		2.384	145870	749090	114650	
Q01082	Spectrin beta chain, non-erythrocytic 1	SPTBN1	sp Q01082 SPTB2_HUMAN Spectrin beta chain, no	120	274.61	2.354		5.0002		1.5658		2.354	14363000	46226000	27935000	
A0A0D95F54;A0A0D95F6;A0A0D95F6;A0A0D95F4;A0	SPTAN1		tr A0A0D95F54 A0A0D95F54_HUMAN Spectrin alpi	132	282.83	2.3502		5.0256		1.4746		2.3502	16833000	62862000	26440000	
P07948;E5R	Tyrosine-protein kinase Lyn	LYN	sp P07948 LYN_HUMAN Tyrosine-protein kinase L	12	58.573	2.3857		2.2951				2.3404	0	1032300	2217900	
Q9UN86;D6	Ras GTPase-activating protein-binding prote	G3BP2	sp Q9UN86 G3BP2_HUMAN Ras GTPase-activating	11	54.12	2.3338		1.3159		2.5495		2.3338	8272900	13070000	6033900	
P07900;G3V	Heat shock protein HSP 90-alpha	HSP90AA1	sp P07900 HS90A_HUMAN Heat shock protein HSP	63	84.659	2.277		4.0858		2.008		2.277	6729400	12647000	4596800	
P46013	Antigen Ki-67	MKI67	sp P46013 KI67_HUMAN Proliferation marker prot	17	358.69	2.3191		2.2468		2.2169		2.2468	524560	475360	44507	
P60228;E5R	Eukaryotic translation initiation factor 3 sub	EIF3E	sp P60228 EIF3E_HUMAN Eukaryotic translation in	25	52.22	2.3804		2.2127		1.9171		2.2127	1089300	1573400	1367200	
P49916;K7E	DNA ligase 3	LIG3	sp P49916 DNL3_HUMAN DNA ligase 3 OS=Homo	8	112.91	2.9178		2.203		2.1767		2.203	1532800	1039900	946440	
Q5RKV6	Exosome complex component MTR3	EXOSC6	sp Q5RKV6 EXOS6_HUMAN Exosome complex con	6	28.235	2.3573		2.1818		2.111		2.1818	11071000	15292000	4620400	
P12931	Proto-oncogene tyrosine-protein kinase Src	SRC	sp P12931 SRC_HUMAN Proto-oncogene tyrosine-	8	59.834	2.168		4.1415		1.8886		2.168	748320	2601200	1702500	
P63092;Q5J	Guanine nucleotide-binding protein G(s) su	GNA3	sp P63092 GNA32_HUMAN Guanine nucleotide-bi	13	45.664	2.1627		4.1417		1.5402		2.1627	1488700	9048500	3740200	
O75531;E9P	Barrier-to-autointegration factor;Barrier-to-	BANF1	sp O75531 BAF_HUMAN Barrier-to-autointegratio	6	10.058	2.1605		2.4895		1.4442		2.1605	167700000	464450000	175040000	
Q9Y265;E7E	RuvB-like 1	RUVBL1	sp Q9Y265 RUVB1_HUMAN RuvB-like 1 OS=Homo	24	50.227	1.8486		2.1597		2.5745		2.1597	2800700	6342500	382330	
O14578;H7E	Citron Rho-interacting kinase	CIT	sp O14578 CTRO_HUMAN Citron Rho-interacting k	11	231.43	3.1776		2.1397		0.96079		2.1397	57864	292140	49921	
P27986;H0Y	Phosphatidylinositol 3-kinase regulatory su	PIK3R1	sp P27986 P85A_HUMAN Phosphatidylinositol 3-k	6	83.597	1.5657		2.1169		2.5085		2.1169	745890	11166000	1210500	
Q6WCQ1;J3	Myosin phosphatase Rho-interacting protei	MPRIIP	sp Q6WCQ1 MPRIIP_HUMAN Myosin phosphatase	12	116.53	2.1049		2.173		0.79734		2.1049	588250	1624600	104110	
P08754	Guanine nucleotide-binding protein G(k) su	GNAI3	sp P08754 GNAI3_HUMAN Guanine nucleotide-bir	15	40.532	2.0157		4.9059		2.0813		2.0813	19273000	75469000	42160000	
O15234;I3K	Protein CASC3	CASC3	sp O15234 CASC3_HUMAN Protein CASC3 OS=Homo	8	76.277	2.067		2.0138		2.7423		2.067	698630	2073400	4126900	
P17987;E7E	T-complex protein 1 subunit alpha	TCP1	sp P17987 TCPA_HUMAN T-complex protein 1 sub	34	60.343	1.5294		2.2873		2.0582		2.0582	485300	1703400	621710	
Q5SRQ6;P6	Casein kinase II subunit beta	CSNK2B;CSN	tr Q5SRQ6 Q5SRQ6_HUMAN Casein kinase II subui	8	26.925	2.0436		2.4349		1.2233		2.0436	5899500	15187000	987590	
P08238;Q5H	Heat shock protein HSP 90-beta	HSP90AB1	sp P08238 HS90B_HUMAN Heat shock protein HSP	64	83.263	1.9891		2.9912		2.02		2.02	7615400	29148000	15600000	
O95425;A0F	Supervillin	SVIL	sp O95425 SVIL_HUMAN Supervillin OS=Homo sap	9	247.74	1.4281		3.0818		2.0134		2.0134	360680	1636100	213390	
Q14676;A2J	Mediator of DNA damage checkpoint protei	MDC1	sp Q14676 MDC1_HUMAN Mediator of DNA dama	20	226.66	2.1653		2.0075		1.5305		2.0075	303620	152960	60101	
Q14008;H0N	Cytoskeleton-associated protein 5	CKAP5	sp Q14008 CKAP5_HUMAN Cytoskeleton-associat	72	225.49	1.7242		2.0021		2.3599		2.0021	325010	2252600	1461800	

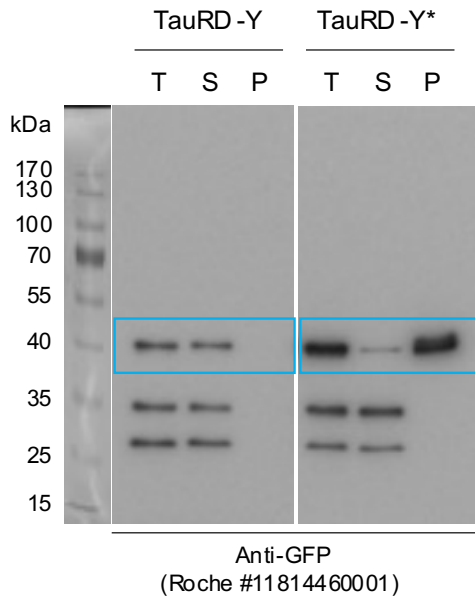
269

270

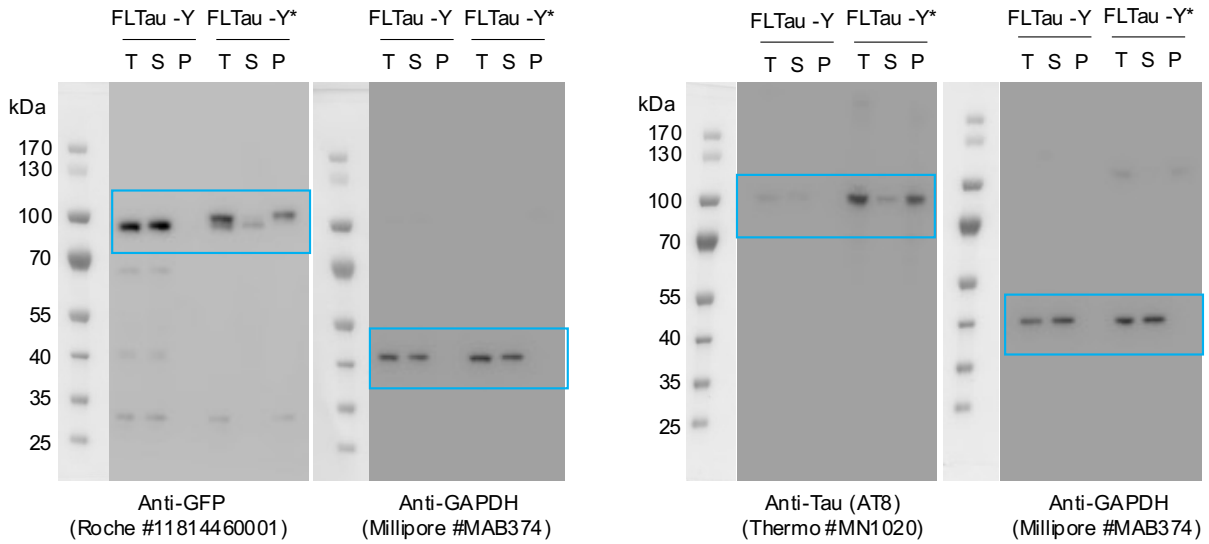
271 **Uncropped scans of blots**

272

Supplementary Fig. 1c

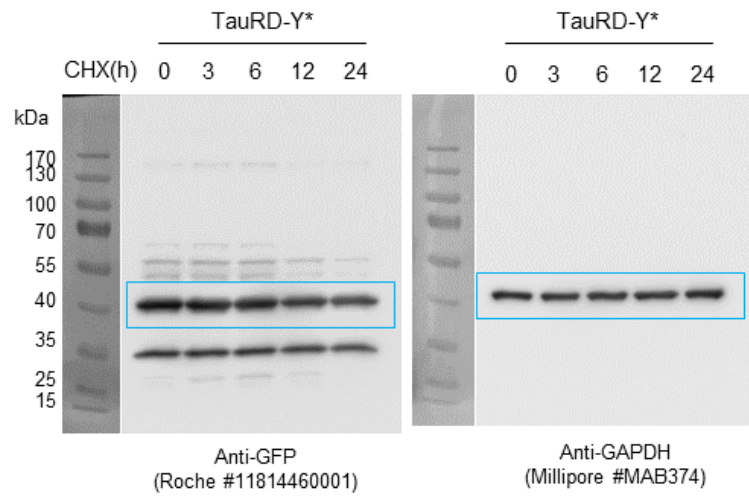
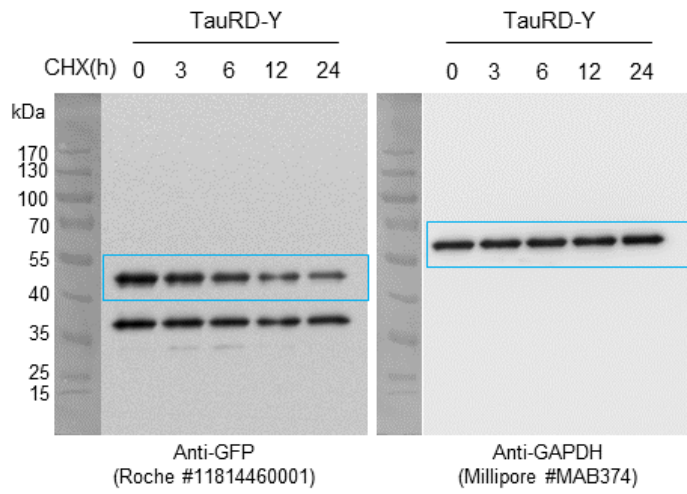


Supplementary Fig. 1e

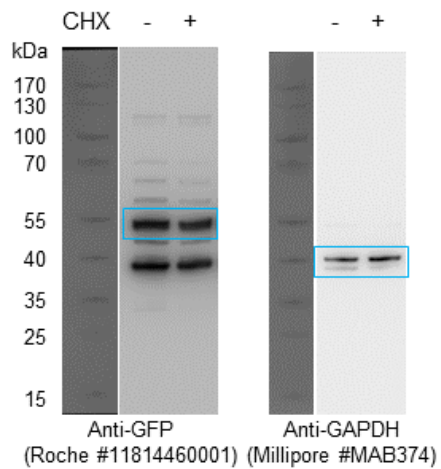


273

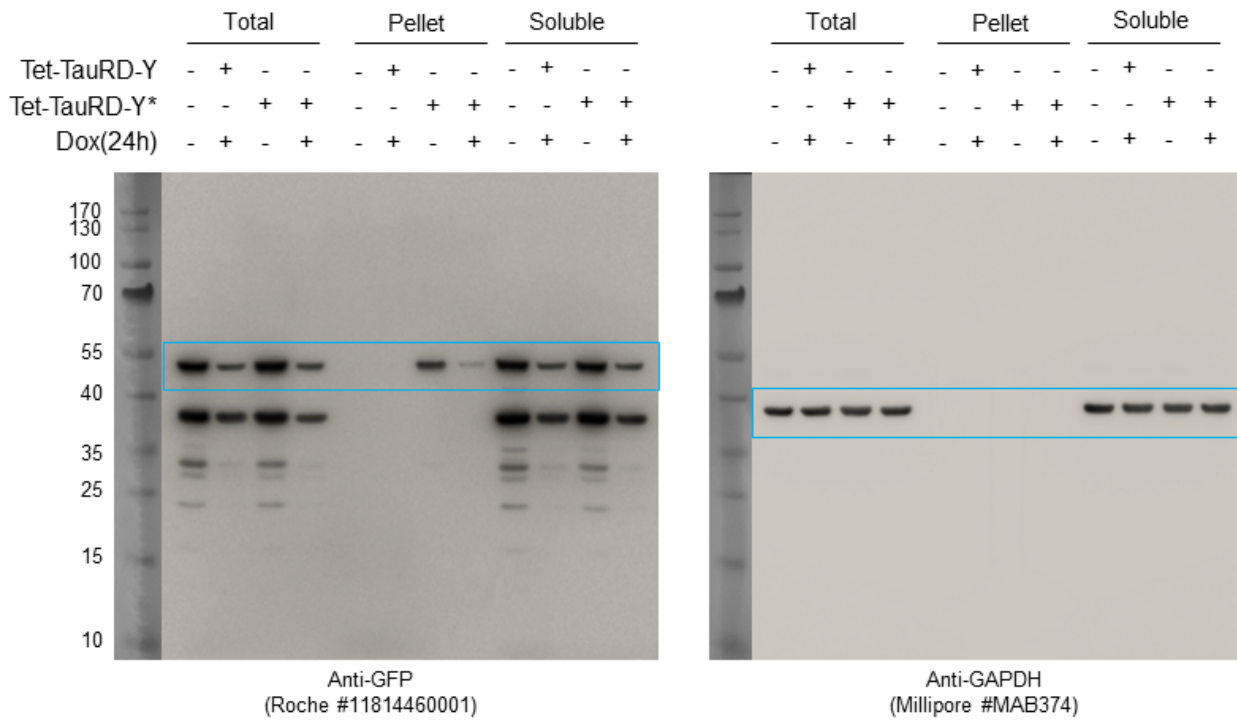
Supplementary Fig. 3a



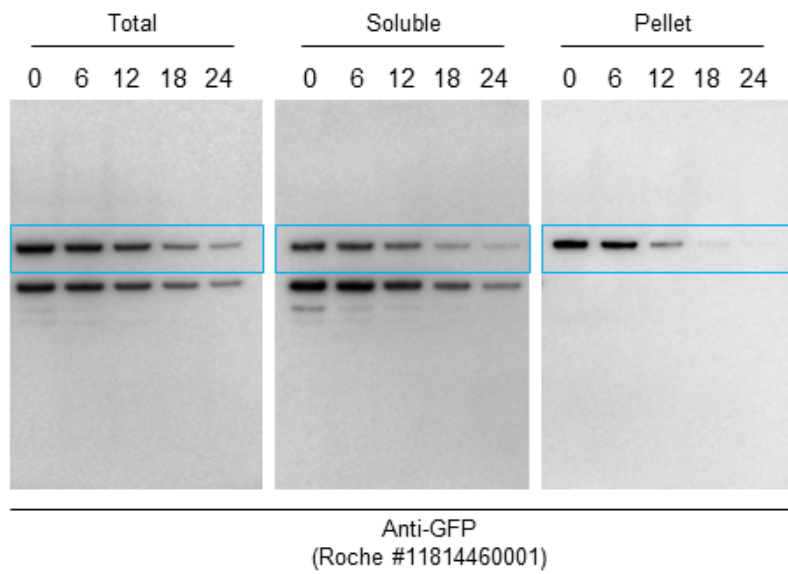
Supplementary Fig. 3b



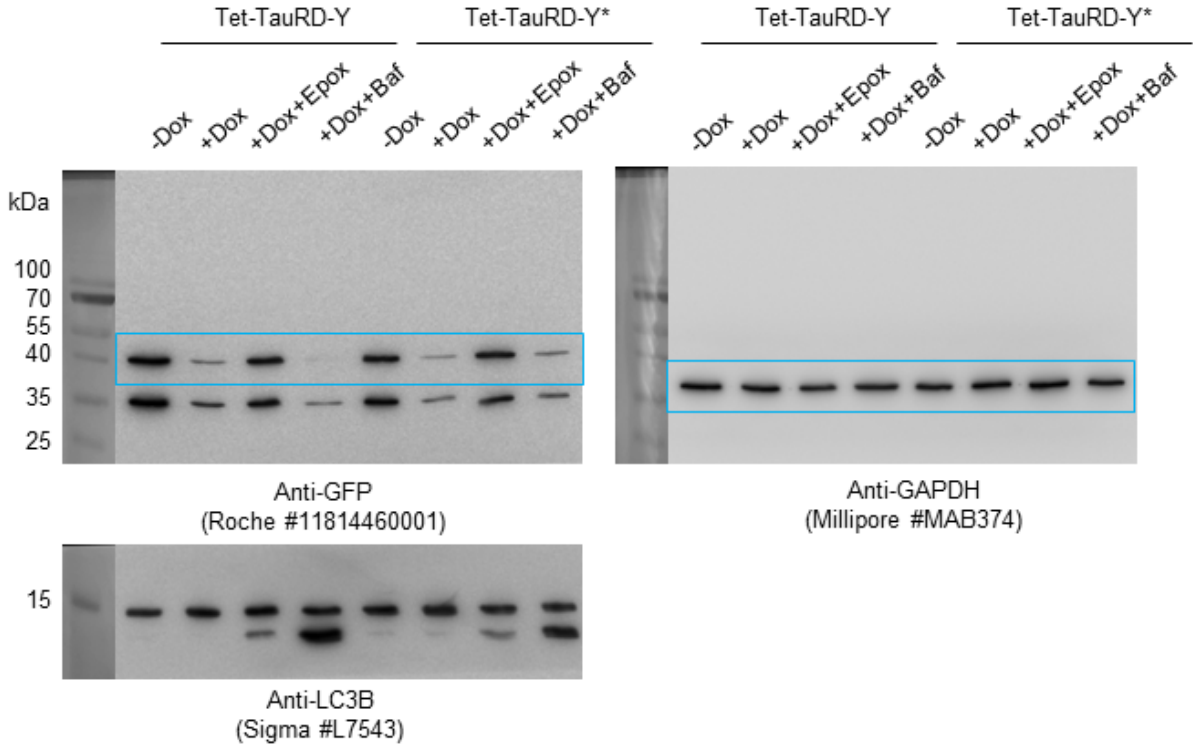
Supplementary Fig. 3c



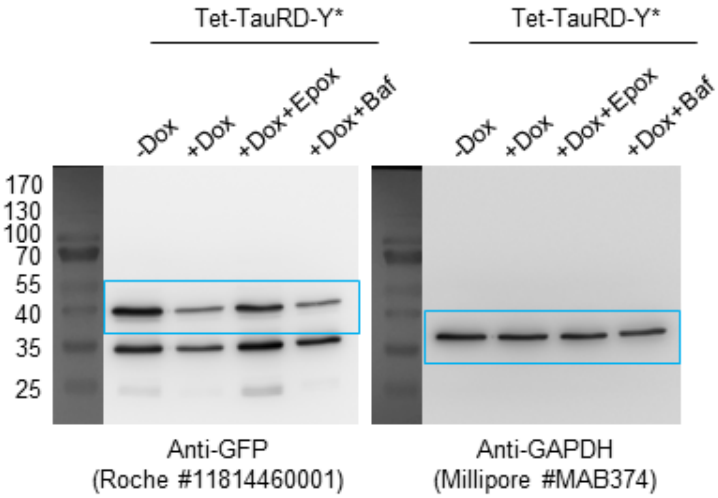
Supplementary Fig. 3c



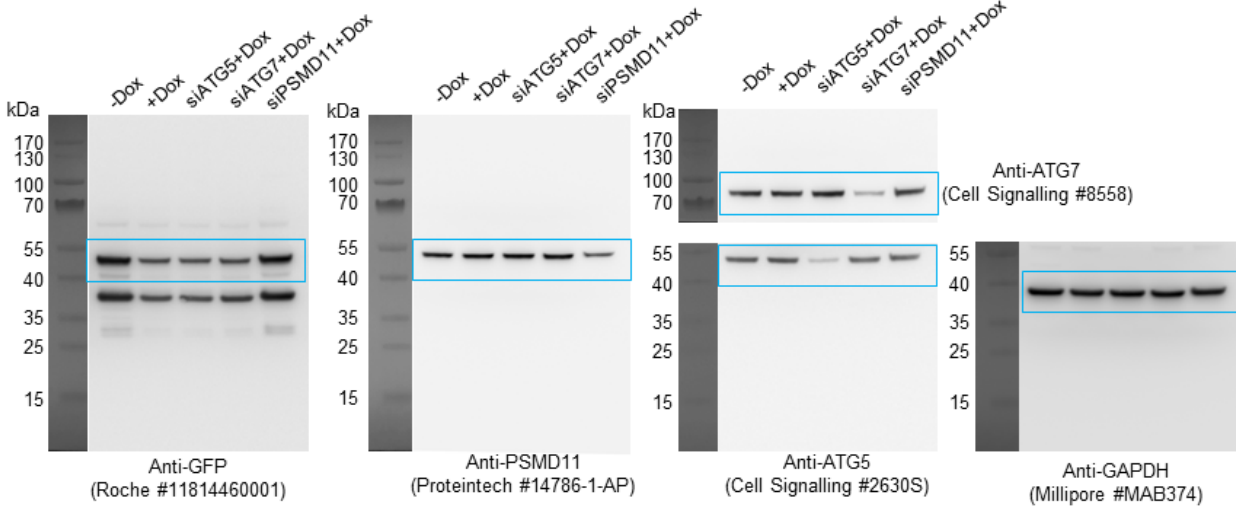
Supplementary Fig. 4a



Supplementary Fig. 4b

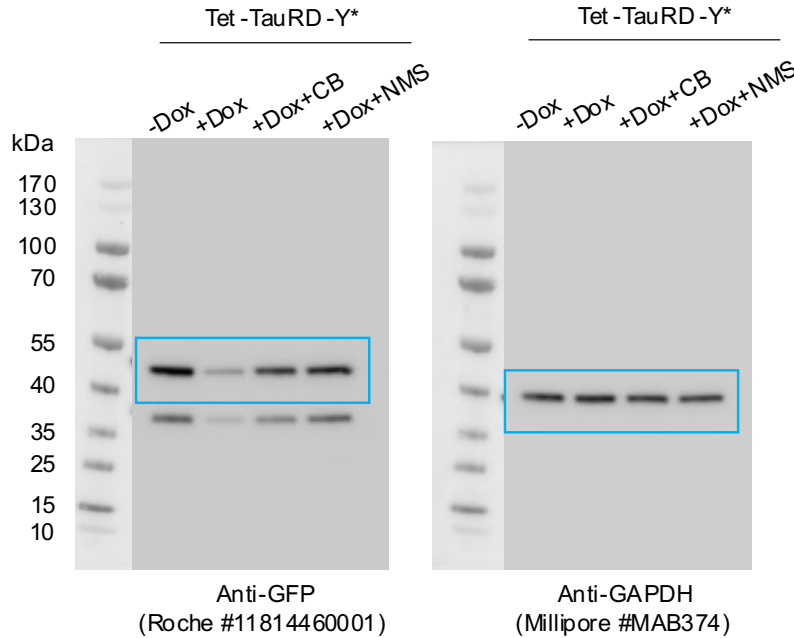


Supplementary Fig. 4e

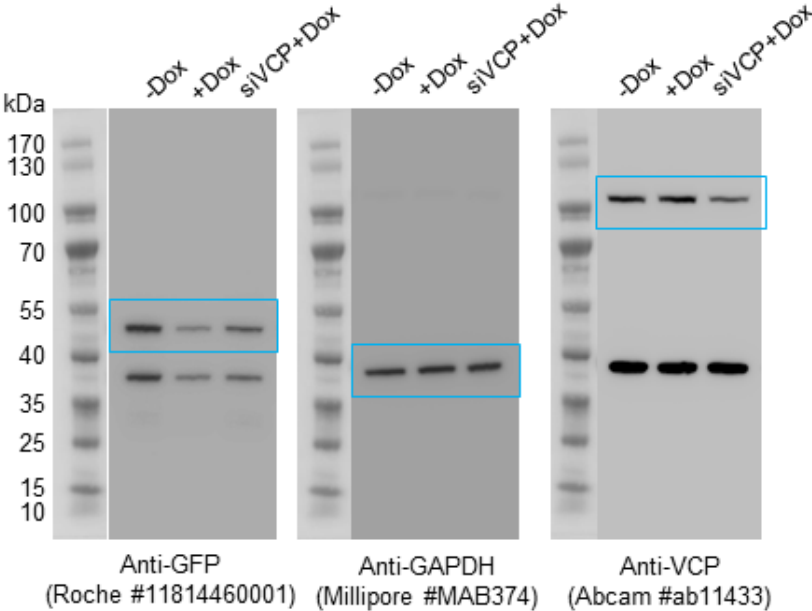


275  
276

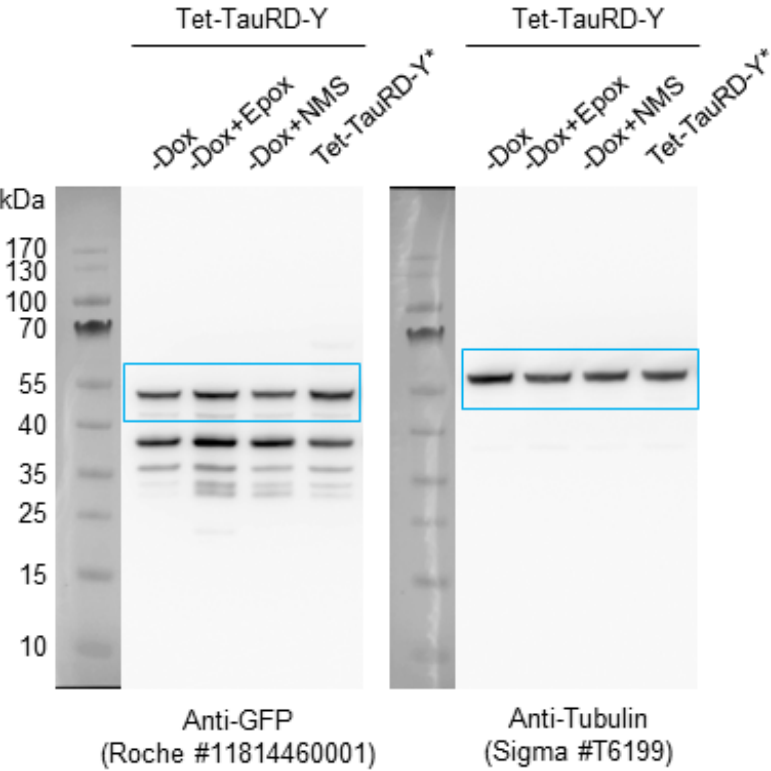
Supplementary Fig. 5e



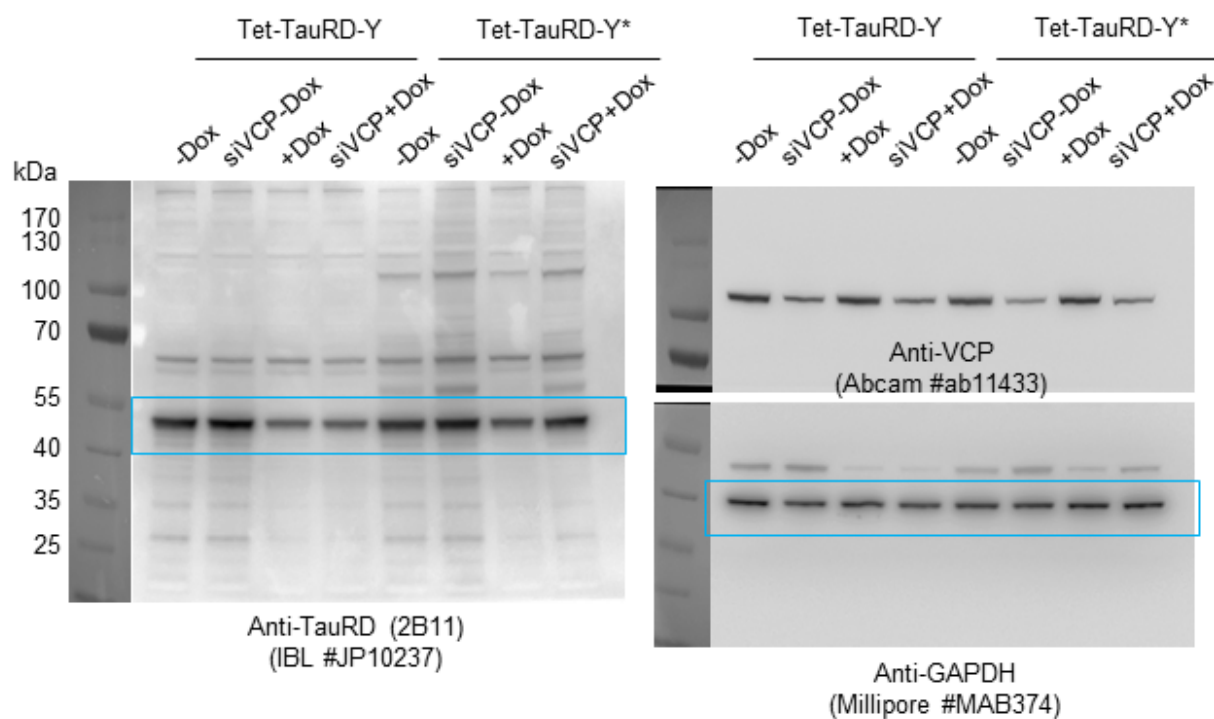
Supplementary Fig. 5g



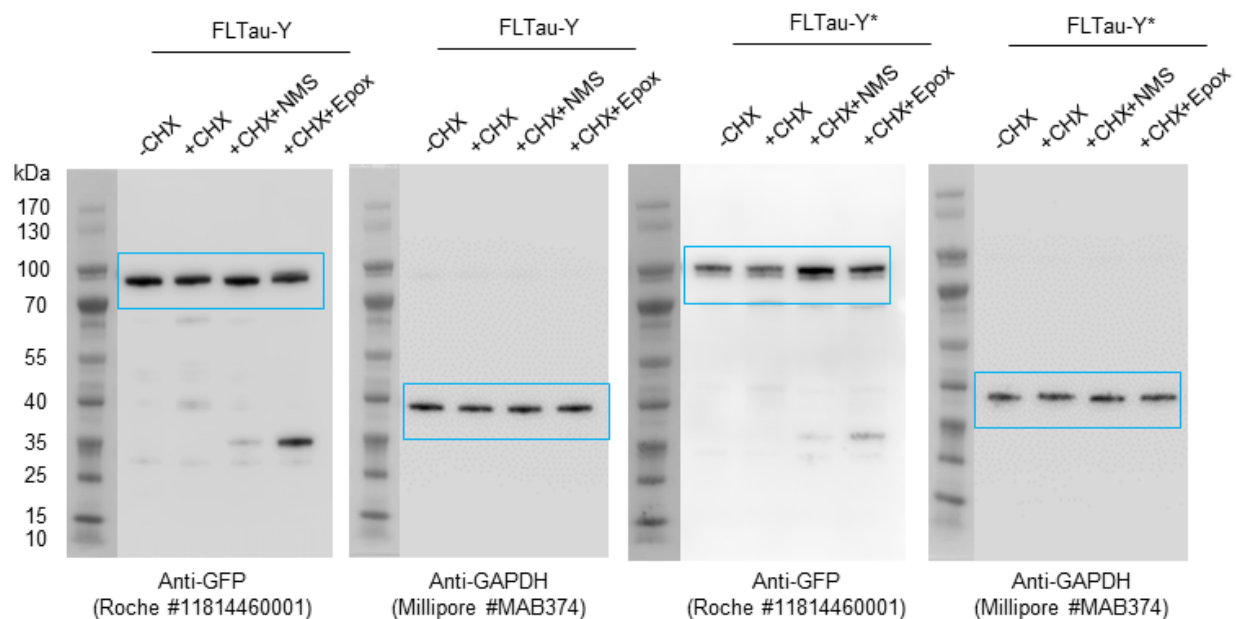
Supplementary Fig. 5i



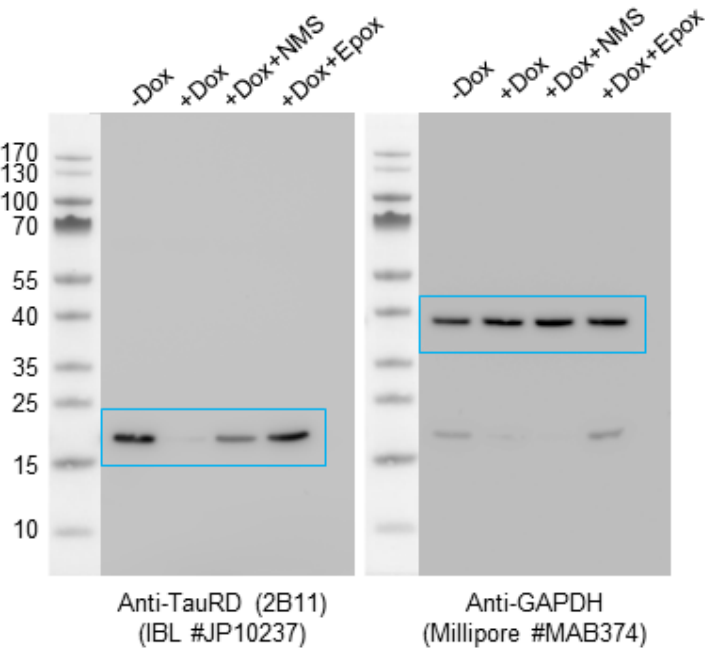
Supplementary Fig. 5k



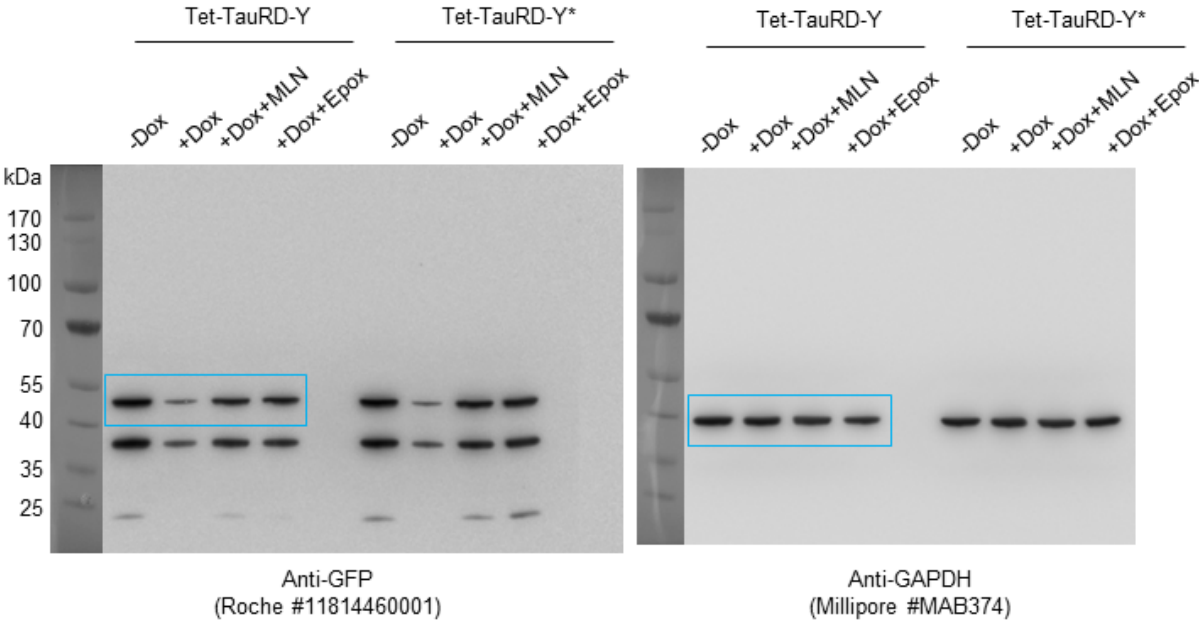
Supplementary Fig. 6c



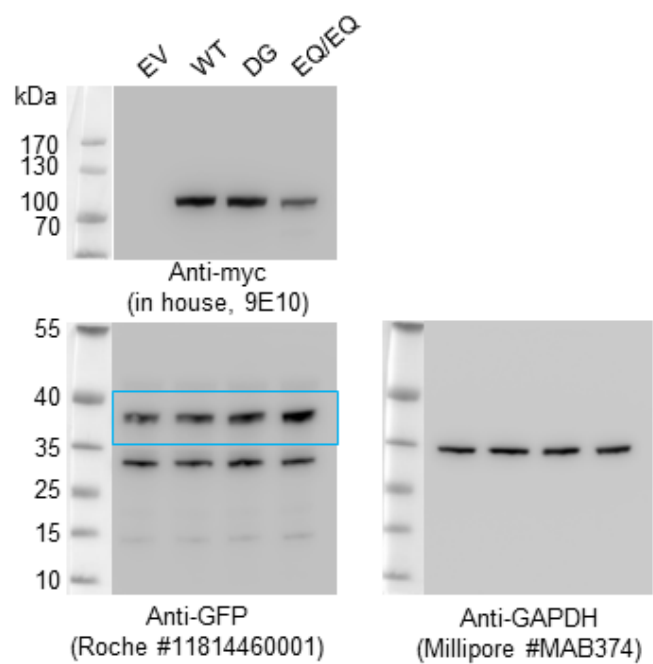
Supplementary Fig. 6e



Supplementary Fig. 8e



Supplementary Fig. 12c



277